Benzoxazinoid-mediated microbiome feedbacks enhance Arabidopsis growth and defense

Katja Stengele[1], Lea Stauber[2], Lisa Thoenen[1,3], Henry Janse van Rensburg[1], Viola D'Adda[1], Klaus Schlaeppi[1]

[1]Department of Environmental Sciences, University of Basel, 4056, Basel, Switzerland; [2]Institute for Infectious Diseases, University of Bern, 3013, Bern, Switzerland; [3]Division of Food Microbial Systems, Agroscope, 3003 Bern, Switzerland

Author for correspondence:

Klaus Schlaeppi

klaus.schlaeppi@unibas.ch

ORCIDs:

KSt: 0009-0008-3843-2868

LS: 0000-0001-8367-6150

LT: 0000-0002-0988-2690

HJvR: 0000-0002-5632-8422

KS: 0000-0003-3620-0875

Manuscript information:

Word count: 6568 total: 192 Summary, 830 Introduction, 2026 Materials & Methods, 1611 Results, 1909 Discussion (6376 words without Summary)

Number of figures: The article comprises 6 main figures, all in color, and 3 supplementary figures.

Number of tables: The article comprises 9 supplementary tables.

Supporting information: separate documents

Summary

- Plants modulate their surrounding microbiome via root exudates and this conditioned soil microbiome feeds back on the performance of the next generation of plants. How plants can perceive this altered microbiome and modulate their performance in response to such microbiome feedbacks however remains largely unknown.
- We made use of two maize lines, which differ in their ability to exude benzoxazinoids, to condition two contrasting soil microbiomes in the same starting soil. Based on these conditioned soils we have established a model system with *Arabidopsis thaliana* (Arabidopsis) to investigate the mechanisms of microbiome feedbacks.
- Arabidopsis plants grown on the benzoxazinoids conditioned soil developed larger rosettes, for which the soil microbiome was required. Arabidopsis roots also harbored differential bacterial communities. Further, these plants showed enhanced defense signatures in their shoot and were more resistant to the fungal pathogen *Botrytis cinerea*.
- We could establish Arabidopsis as a model to study benzoxazinoid-mediated microbiome feedbacks, which will allow future studies to investigate underlying mechanisms. Arabidopsis also responded with both improved growth and enhanced resistance to a complex benzoxazinoids conditioned microbiome, and we hypothesize that this simultaneous increase of growth and defense is mediated by priming of defenses.

Keywords

Arabidopsis thaliana, *Botrytis cinerea*, microbiome feedback, plant-soil feedback, root microbiota, secondary metabolites

Introduction

Plants condition the surrounding soil throughout their life-time to optimize their immediate environment by changing the biotic and abiotic properties of the soil they grow in (van der Putten *et al.*, 2013). These soil changes also persist and influence the performance of a next generation of plants, which is known as a plant soil feedback (PSF; Bezemer *et al.*, 2006; van der Putten *et al.*, 2013; Mariotte *et al.*, 2018). In the conditioning phase of PSFs, the growing plants alter not only the physiochemical soil properties such as soil structure, organic matter content or nutrient levels, but they also alter the specific metabolite profile (Delory *et al.*, 2024), and the biotic soil properties including the soil microbiome (Semchenko *et al.*, 2022; Jing *et al.*, 2022). The responses to these soil alterations then "feed" back on the growth and/or defense of the next plant generation. If these feedbacks can be specifically assigned to altered soil microbiomes, which the plant perceives and responds to, we refer to them as 'microbiome feedbacks' (Janse van Rensburg *et al.*, 2024).

The microorganisms living in soil also present the majority of the microorganisms that colonize plant roots (Spooren *et al.*, 2024). These microorganisms collectively function as a microbiome, which includes bacteria, fungi, viruses and protists (Bai *et al.*, 2022). This root microbiome affects plant health and performance (Bulgarelli *et al.*, 2013; Trivedi *et al.*, 2020), for example by regulating plant nutrient homeostasis (Salas-González *et al.*, 2021), mitigating abiotic stress (Schmitz *et al.*, 2022) or protecting from pathogens (Durán *et al.*, 2018). To foster such beneficial interactions, plants can selectively modulate the composition and activity of their root and surrounding soil microbiome through the secretion of root exudates (Sasse *et al.*, 2018; Jacoby *et al.*, 2021). These exudates include primary and secondary metabolites, which act as food sources or specific communication cues to microbes (Sasse *et al.*, 2018; Korenblum *et al.*, 2022). Several specific classes of exuded metabolites have been demonstrated to modulate the plant root and rhizosphere microbiota, including coumarins (Stringlis *et al.*, 2018), flavones (Yu *et al.*, 2021), and benzoxazinoids (Hu *et al.*, 2018; Cotton *et al.*, 2019; Kudjordjie *et al.*, 2019).

Benzoxazinoids (BXs) are indole-derived alkaloids that function as secondary metabolites, and they are mainly produced by *Poaceae*, including maize, wheat and rye (Niemeyer, 2009; Niculaes *et al.*, 2018). BXs are multifunctional and act for instance in the aboveground defense against generalist herbivores (Wouters *et al.*, 2016; Robert & Mateo, 2022). BXs are also exuded in substantial amounts into soil, particularly by maize (Hu *et al.*, 2018), where the main exuded metabolite is 2,4-dihydroxy-7-methoxy-1,4-benzoxazin-3-one (DIMBOA). DIMBOA is spontaneously converted into 6-methoxybenzoxazolin-2(3H)-one (MBOA) in soil, which is then further metabolized to 2-amino-7-methoxyphenoxazin-3-one (AMPO) by microbes (Niemeyer, 2009). In soil, BXs have important belowground functions with their allelopathic effects on neighboring or successional plants (Teasdale *et al.*, 2012; Schandry & Becker, 2020). Typical phytotoxic compounds are the BX breakdown products

2-amino-3H-phenoxazin-3-one (APO) and AMPO, which have been shown to inhibit growth of Arabidopsis *in vitro* (Venturelli *et al.*, 2015).

BXs also have important belowground functions on the microbiota in PSFs. The root and rhizosphere microbiotas are selectively shaped by the exuded BXs, which leaves a legacy in soil for a next plant generation (Hu *et al.*, 2018; Cotton *et al.*, 2019; Kudjordjie *et al.*, 2019). This BX-dependent soil conditioning was found to affect the growth and the defense of a next generation of maize (Hu *et al.*, 2018) or wheat (Cadot *et al.*, 2021). Sterilization and microbiota complementation experiments demonstrated that these feedbacks were BX-dependent and mediated by the microbes. Hereafter, we refer to these PSFs as 'BX-feedbacks'. To study BX-feedbacks, we compare soil conditioned with wild-type maize plants that exude BXs, called 'BX_{plus}' soil, to control 'BX_{minus} soil' that is conditioned by the BX-defective mutant line *bx1* (Maag *et al.*, 2016). While the phenology (Hu *et al.*, 2018; Cadot *et al.*, 2021) and the agronomic relevance (Gfeller *et al.*, 2023b,a) of BX-feedbacks have been extensively described, the mechanistic understanding of how plants perceive a BX_{plus} soil and how they alter their own performance remains largely unknown. And in more general terms, how plants perceive complex soil microbiomes and how they mediate microbiome feedbacks, is currently understudied (Janse van Rensburg *et al.*, 2024).

To facilitate mechanistic studies, we explored BX-feedbacks with the model plant *Arabidopsis thaliana* Col-0 (henceforth Arabidopsis) which we grew on BX_{plus} and BX_{minus} soils. Arabidopsis robustly responded with increased shoot growth on BX_{plus} soil. Through soil sterilization, we showed that the soil microbiota is required for this growth feedback. BX-conditioning also lead to different bacterial communities on Arabidopsis roots. A transcriptome analysis revealed upregulation of defenses in shoots, which was corroborated with smaller lesions of the pathogen *Botrytis cinerea* when plants were grown on BX_{plus} soil. In conclusion, with the newly established model system to study BX-feedbacks we uncovered that a BX_{plus} microbiota leads to enhanced growth in Arabidopsis and most likely primes the plant's defenses, explaining the better resistance to *B. cinerea*.

Materials and Methods

Plant material

For the soil conditionings, we used the maize (*Zea mays* L.) variety B73 and the benzoxazinoid-deficient line *bx1*, a transposon insertion mutant in B73 background (Maag *et al.*, 2016). For the feedback experiments, we used *Arabidopsis thaliana* Col-0 seeds.

Soil conditioning

We collected soil from two neighbouring fields managed by Agroscope in Changins (Nyon, Switzerland) between 2019 and 2022 to condition it with maize. Soils were sieved (1 cm mesh size), homogenized, and stored at 4°C before conditioning. For each conditioning event, which yields one "soil batch", we grew wild-type B73 and *bx1*(B73) maize for 12 weeks in individual pots. For details on the set up of each conditioning experiment, see **Table S1**. Plants were watered three times a week and supplemented once a week with nutrient solution (**Table S1**). After twelve weeks, the roots were removed from the pots and the soils were collected and pooled by maize genotype, resulting in BX_{plus} soil (i.e., conditioned with B73 wild-type maize) and BX_{minus} control soil (i.e., conditioned with *bx1*(B73) maize). Soils were stored at 4°C until further use.

Arabidopsis experiments on soil

We have performed several Arabidopsis experiments (Exp. I to Exp. X) with slightly different setups, which are detailed in **Table S2**. As a general procedure to perform Arabidopsis experiments, the conditioned soils were sieved (5 mm mesh size), amended with 20% (v/v) autoclaved sand and filled to the same weight into small pots. For experiment III, fractions of the soil/sand mixtures were sterilized by X-radiation (36 – 40 kGy, Synergy Health AG, Däniken, Switzerland) before filling to pots. Arabidopsis seeds were stratified for 2-3 days either directly on the pots or suspended in 0.2% sterile agar before sowing. For experiment III, seeds were sterilized (described below for MBOA Experiment II). Several seeds were distributed per pot, and after 1-2 weeks, the healthiest looking seedling was kept and the others were removed from the pot. Plants were grown in growth cabinets (Percival, CLF Plant Climatics, Wertingen, Germany) at 60% relative humidity, 10 h day at 21°C and light intensities between 100 and 200 µmol m^{-2} s^{-1}, and 14 h night at 18°C. Pots were watered with tap water or autoclaved tap water (Exp. III) three times per week based on weight, and the pot position was changed once per week. Plants were fertilized once or twice during the growth phase (except for Experiments I and VI), by watering with 1:2 diluted ½ strength Hoagland solution (Cardoso *et al.*, 2014). Plants were grown for six to seven weeks before harvesting. Rosette area was determined by either analyzing scans of cut rosettes with ImageJ v1.5 (Schneider *et al.*, 2012), or by analyzing photographs of rosettes from living plants with the software ARADEEPOPSIS (Hüther *et al.*, 2020).

Arabidopsis experiment on agar plates

We have performed two experiments on agar plates, where plants were grown in Percival growth chambers (growth settings described under *Arabidopsis experiments on soil*). For the MBOA experiment I, seeds were sterilized for four hours with chlorine gas **(**Lindsey III *et al.*, 2017), and then directly sown to ½ Murashige and Skoog (MS; Duchefa, Haarlem, the Netherlands) plates containing 1.5% plant agar (Duchefa, Haarlem, the Netherlands) supplemented with MBOA (Sigma-Aldrich, St. Louis, USA) at different concentrations (100, 500 or 1000 µM) or no MBOA as control. MBOA was dissolved in DMSO (Sigma-Aldrich), which was kept constant at 500 µL per L ½ MS agar in each treatment including the control. 12 to 16 seeds were sown per plate and stratified for three days at 4°C. Seed germination was recorded for the first four days after germination, and primary root length was quantified ten days after sowing.

For the MBOA experiment II, seeds were surface sterilized with 70% Ethanol + 0.1% Triton-X100 for 1 minute, Javel water + 0.1% Triton-X100 for 12 minutes, and washed three times with sterile milliQ water. Seeds were sown onto ½ MS agar plates containing 1% sucrose, stratified for three days at 4°C and germinated for eight days. The seedlings were then transferred to ½ MS plates containing 825.75 µL DMSO per L ½ MS agar as control or plates containing the same amount of DMSO with different MBOA concentrations (50, 100 or 500 µM). Five seedlings were transferred onto each plate and grown for additional 13 days, before the total root and shoot material per plate was harvested to determine the fresh weight.

Infections with *Botrytis cinerea*

For infections, the *Botrytis cinerea* strain B05.10 was grown in the dark at 18°C on potato dextrose agar (Merck Millipore, Burlington, USA) for two to three weeks. Plants were grown as described under *Arabidopsis experiments on soil*. At six to seven weeks, three mature source leaves per plant were infected with *B. cinerea* spores that were harvested from plates with sterile water + 0.0001% Tween-20 (Biorad, Basel, Switzerland), filtered through glass wool, and adjusted to $1x10^5$ spores per mL in ½ strength potato dextrose broth (Formedium, Norfolk, United Kingdom). For infection, a 5 µL drop was placed onto the middle of the leaf towards the edge. The plant trays were covered with a water-sprayed transparent lid that was taped to the tray to ensure high humidity. For the infection, plants were transferred to a growth chamber (Sanyo, Moriguchi, Japan) at the same growth conditions as previously, but equipped with fluorescent bulbs of ~ 100 µmol m^{-2} s^{-1} light intensity. The area of the lesions was quantified with the Fiji distribution of Image J (Schindelin *et al.*, 2012) three days after infection.

Determination of benzoxazinoid concentrations in soils

Before the first Arabidopsis experiments, soil samples of soil batches 1, 2 and 4 were stored at -80 °C, to analyse the BX concentrations following the sample processing and analysis described in Gfeller et al. (2023b). Briefly, BXs were extracted with acidified Methanol (70% Methanol, 0.1% formic acid),

and analysed in an Acquity UHPLC system coupled to a QToF mass spectrometer without further concentration of samples. Pure BX compounds as described in Gfeller et al. (2023b) were used to determine absolute quantities via calibration curves.

Microbiota profiling

For the microbiota profiling of experiment III, we analysed the bacterial and fungal communities of roots grown in native and sterilized soils along with native soil samples. The soil samples were taken from the middle of unplanted pots that had been included in experiment III, and adjusted to approximately 250 mg. For roots, we harvested them from the pot and sampled a 5 cm long root fragment starting from 1 cm below the rosette base. These root segments were washed in 10 mM $MgCl_2$, blot dried with tissue paper, snap frozen in liquid nitrogen, and stored at -80°C. Root samples were then lyophilized (FreeZone Plus; Labconco Corporation, Kansas City, USA) for three days and grinded for 5 minutes with a ball mill (Mixer Mill MM 400; Retsch GmbH, Haan, Germany). From all samples, we extracted the DNA with the NucleoSpin Soil DNA extraction kit (Macherey-Nagel, Düren, Germany), and quantified the DNA concentrations with the AccuClear® Ultra High Sensitivity dsDNA Quantitation Kit (Biotium, Fremont, USA). We normalized the concentration to 0.2 ng/µL for soil samples and 2 ng/µL for root samples, or used undiluted samples if DNA concentrations were lower.

Next, we performed two-step PCR amplification and barcoding of the bacterial 16S gene region and the fungal ITS spacer region as was previously described in Gfeller et al., (2023b). We used the same cycling profiles, but with 3 minutes of initial denaturation. The reaction of the first 16S PCR was composed of 1x 5Prime HotMasterMix (Quantabio, Beverly, USA), 0.3% BSA, 300 nM of each primer and 10 ng root DNA or 1 ng soil DNA. The second PCR contained 6 µL of purified PCR product (using SPRIselect beads; Beckman Coulter Life Sciences, Indianapolis, USA) and individual barcoded primer pairs for each sample. The ITS PCR reactions contained 200 nM of each primer but were otherwise the same as the 16S reactions. The products from the second PCR were then purified with SPRIselect beads, and pooled to 25 ng DNA per sample for the 16S samples, and to 2.5 ng DNA or as much as was available per sample for the ITS samples. Both pools were bead purified again and pooled for the final library.

The library was sequenced with the MiSeq reagent kit v3 at the Next Generation Sequencing Platform (University of Bern) using the 2x 300 bp pair-end sequencing protocol (Illumina Inc., San Diego, USA). The MiSeq 16S and ITS reads were quality checked with FastQC v0.11.8 (Babraham Institute, Cambridge, United Kingdom) and demultiplexed with cutadapt v2.10 (Martin, 2011). Quality filtering, read merging and amplicon sequence variants (ASV) clustering was implemented in R v4.0.0 (R Core Team, 2017) using the R package dada2 v1.16.0 (Callahan *et al.*, 2016). Bacterial taxonomies were assigned with a naïve Bayesian classifier using a DADA2 formatted training set (silva_nr_v132_train_set.fa.gz) from the SILVA database (Quast *et al.*, 2013), and fungal taxonomies

were assigned with a training set (sh_general_release_dynamic_02.02.2019.fasta) from the UNITE database (Abarenkov *et al.*, 2024).

In R v4.3.0 (R Core Team, 2017), we removed reads assigned to Eukarya, Archaea, Cyanobacteria or Mitochondria from the bacterial ASV count table. Due to low read numbers, we removed 11 samples from the ITS library that had less than 900 reads. We normalized both libraries with total sum scaling and did not rarefy the libraries, as the number of reads did not differ between sample groups (Weiss *et al.*, 2015). We ran data ordinations based on Bray-Curtis dissimilarity matrices (Bray & Curtis, 1957) using the R package phyloseq v1.44.0 (McMurdie & Holmes, 2013) and visualized them with unconstrained Principal Coordinate Analysis (PCoA). We performed Permutational Multivariate Analysis of Variance (PERMANOVA) with 99'999 permutations with the adonis function from the vegan package to partition and quantify effects of our experimental factors. To determine differentially abundant ASVs, we used four different identification methods, implemented in the R packages ALDEx2 v1.32.0 (Fernandes *et al.*, 2013, 2014), Maaslin2 v1.14.1 (Mallick *et al.*, 2021), metagenomeSeq v1.42.0 (Paulson *et al.*, 2013), and ANCOMBC v2.2.0 (Lin & Peddada, 2020). We defined an ASV to be differently abundant if it was detected by at least three of the four methods. All R-code is documented at https://github.com/PMI-Basel/Stengele_et_al_At_BX-feedbacks.

Transcriptome analysis

Arabidopsis root and shoot sample material were collected for the RNAseq analysis of seven-week-old plants from Experiment V.II. Whole shoots were directly frozen in liquid nitrogen, and the whole roots were collected and removed from all loosely attached soil before freezing. The RNA was extracted with the NucleoSpin RNA kit (Macherey-Nagel, Düren, Germany) and quantified via Fluorometry. Next, RNA quality was checked with TapeStation, and prepared as a library with 200 ng total RNA input using polyA enrichment with the TruSeq Stranded mRNA kit (Illumina, SanDiego, USA). The library was sequenced with a 2x 51 bp paired-end protocol with Illumina NovaSeq6000 (Illumina, San Diego, USA) at the Genomics Facility Basel (https://bsse.ethz.ch/genomicsbasel).

After quality control, reads were aligned to the Arabidopsis thaliana TAIR10 reference genome and read count was performed using STAR 2.7.9a (Dobin *et al.*, 2013). All raw data processing was performed at sciCORE (http://scicore.unibas.ch/) scientific computing core facility at University of Basel. Downstream analyses were performed with R 4.3.0 using DESeq2 v1.42.1 (Love *et al.*, 2014) for differential gene expression analysis. We considered genes to be differentially expressed if the adjusted P value (P_{adj}) < 0.05 and log2FoldChange > ±1. Co-expressed genes were identified using the R package coseq v1.24.0 (Rau & Maugis-Rabusseau, 2018). Models were rerun 20 times to determine the optimal number of clusters. Genes with conditional cluster membership probabilities ≥0.95 and P_{adj} < 0.01 were then used for cluster-wise gene ontology (GO) enrichment analysis using hypergeometric testing, as implemented in the R-package clusterProfiler v4.10.0 (Wu *et al.*, 2021). The full RNAseq analysis pipeline can be found at https://github.com/PMI-Basel/Stengele_et_al_At_BX-feedbacks.

General statistical analyses

All statistical analyses were executed in R v4.3.0 (R Core Team, 2017) within Rstudio v2023 (Posit team, 2023). Rosette area or biomass data were statistically compared between two groups using two-sided t-tests, and correlations were assessed with Pearson correlation tests. Analysis of variance test was used to compare more than one group. All R-code used for statistical analysis and graphing is available from https://github.com/PMI-Basel/Stengele_et_al_At_BX-feedbacks.

Results

Benzoxazinoid-dependent soil conditioning affects Arabidopsis growth

In search of a model system to investigate BX-feedbacks, we tested *Arabidopsis thaliana* Col-0 (hereafter, Arabidopsis) and asked if BX-conditioned soils would lead to differences in growth. We grew Arabidopsis plants in individual pots containing control 'BX_{minus} soil' or BX-conditioned 'BX_{plus} soil'. We observed that plants developed larger rosettes when grown on BX_{plus} compared to the control BX_{minus} soil (**Fig. 1a**). This observation was confirmed using image-based quantification of the rosette area (**Fig. 1b**) and was also reflected in the fresh and dry biomass (**Fig. 1c**). Because rosette area and shoot biomass measures strongly correlated with each other (**Fig. S1a**), we employed the non-destructive image quantifications for the rest of the study. The positive BX-feedback on growth was reproducible with varying setups conducted with independently conditioned soil batches (**Fig. S1b, Table S2**). We also confirmed the accumulation of MBOA and AMPO in BX_{plus} soil, while we could not detect these BXs in BX_{minus} soil (**Fig. S2a**). To investigate if BX-feedbacks also affect root growth, we measured root biomass in two experiments. Of note, weight-based biomass measurements of roots are less accurate than shoot biomass measurements, as a uniform harvest of the entire root system is notoriously difficult from soil. We found a tendentially higher root biomass on BX_{plus} soil (**Fig. 1d**), which also correlated positively with shoot area (**Fig. 1e**). Taken together, Arabidopsis Col-0 responds with increased growth on BX_{plus} soil compared to when grown on BX_{minus} soil.

The soil microbiota mediates Arabidopsis growth differences

In previous work with maize we found that the soil microbiota was driving the BX-feedbacks based on a sterilization experiment (Hu *et al.*, 2018). To also test for this with Arabidopsis, we sterilized BX_{minus} and BX_{plus} soils using X-radiation. Compared to the unsterilized, i.e. the native soils, Arabidopsis grew overall larger on the sterilized soils (**Fig. 2a**), which is mainly explained by nutrient release from sterilization. The better growth on native BX_{plus} soil was no longer seen on sterilized soils, supporting the idea that soil biotic factors drive Arabidopsis BX-feedbacks. Instead, plants grew smaller on sterilized BX_{plus} compared to sterilized BX_{minus} soil. This suggested that Arabidopsis growth is reduced by a factor contained in sterilized BX_{plus} soil. The primary candidates for this factor are the BXs, as both MBOA and AMPO levels were not affected by the sterilization (**Fig. S2a**), and AMPO is known for its allelopathic properties against plants including Arabidopsis (Venturelli *et al.*, 2015, 2016). Thus, we also tested whether Arabidopsis is sensitive to MBOA in sterile settings, as it would be the case at the beginning on the sterilized soil. Seed germination was delayed on MBOA in a dose-dependent manner (**Fig. 2b**), and root length of seedlings was strongly reduced on 500 µM MBOA or higher (**Fig. S1b**). Shoot biomass of three-week-old plants was also reduced by MBOA in a dose dependent manner (**Fig. 2c**) and root biomass was reduced on 500 µM MBOA (**Fig. S1c**). These findings revealed that Arabidopsis growth can be reduced by MBOA under sterile conditions in vitro. Taken together, the

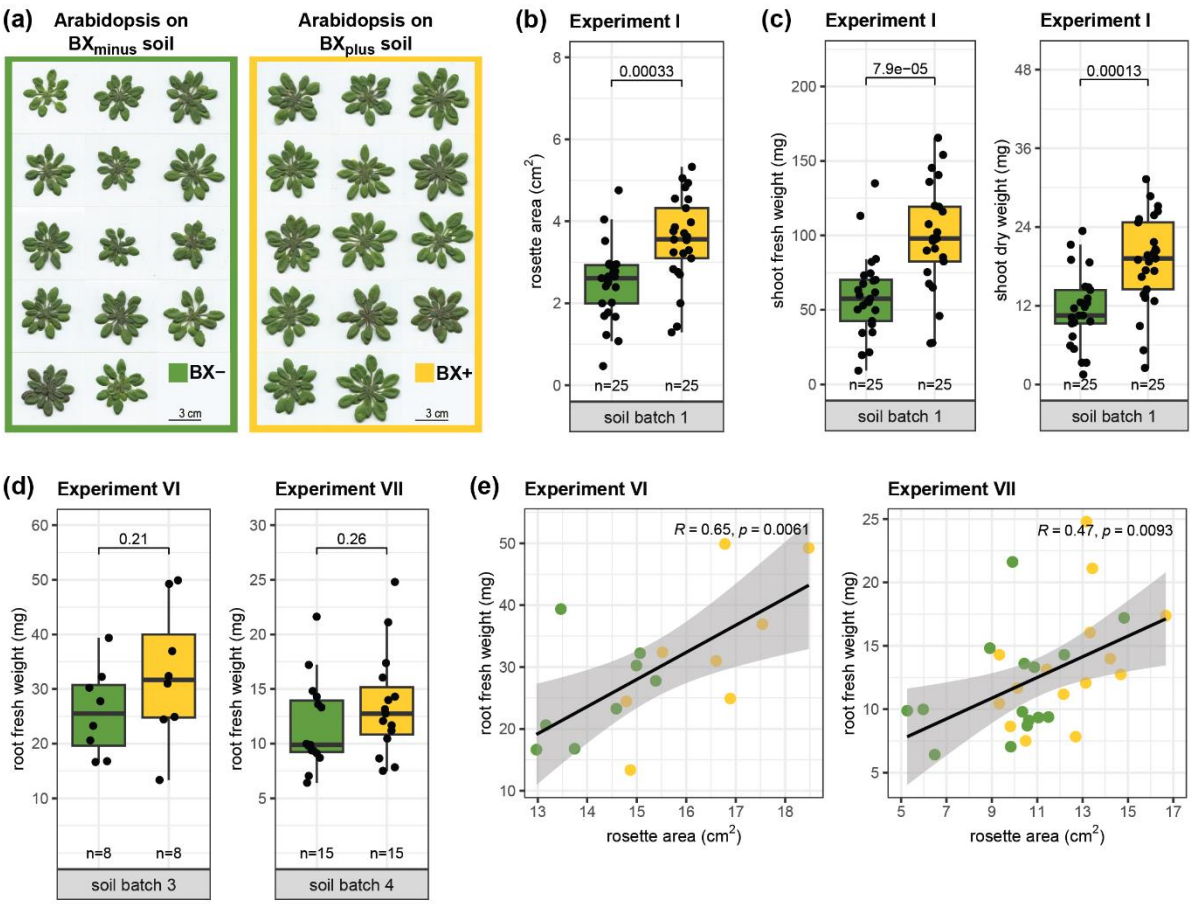

Figure 1 Arabidopsis growth is improved on BX_{plus} compared to BX_{minus} soil. (a) Harvested and scanned shoots of *Arabidopsis thaliana* Col-0 plants grown on BX-conditioned BX_{plus} or on control BX_{minus} soil. Photographs are from Experiment IV. **(b)** Shoot area of Arabidopsis plants grown for seven weeks on BX_{plus} and BX_{minus} soils. **(c)** Shoot biomass shown both as fresh weight and dry weight. The soil batch number, indicated at the bottom of each individual plot, denotes the independent conditioning events of the soil by growing maize plants. **(d)** Root fresh weights of Arabidopsis from two experiments together with their **(e)** correlations with their shoot area data. The pearson correlation coefficients and respective P values are displayed within the plots. Boxplots furhter report the P values of two-sided student's t-tests and the replicate numbers of the different experiments.

better growth of Arabidopsis on native BX_{plus} compared to BX_{minus} soil is reversed if these soils had been sterilized. This might be due to allelopathic effects of AMPO and MBOA in sterilized BX_{plus} soil, whereas such allelopathic effects might be masked by growth promoting effects of the microbiota in native BX_{plus} soil.

Soil and Arabidopsis root microbiota compositions are differentiated by BX-conditioning

Our previous work had also shown that differential microbiotas assembled on roots of maize plants when grown on BX_{minus} or BX_{plus} soils (Hu *et al.*, 2018). To test for this with Arabidopsis, we profiled bacterial and fungal communities on roots and soil collected from the sterilization experiment (**Fig. 2a**). We have also profiled the root microbiotas of the roots grown in the sterilized soils. The idea was that, although the plants started to grow on sterile soil, the roots will become recolonized by microbes during

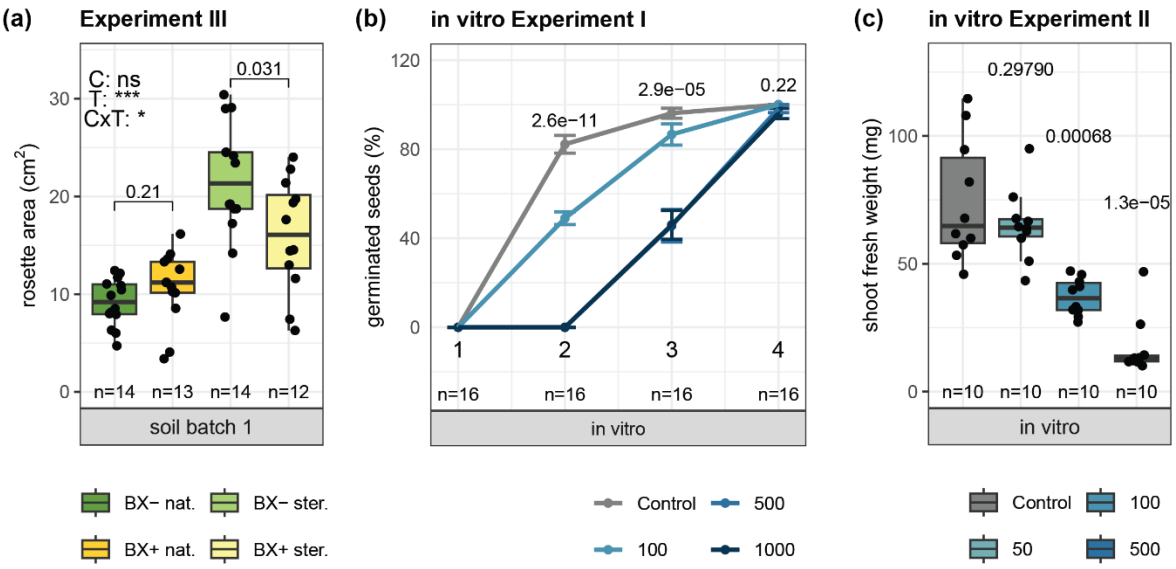

Figure 2 Arabidopsis no longer displays a positive growth feedback on sterilized soil and is sensitive to MBOA. (a) Shoot area of Arabidopsis plants grown on native and sterilized BX_{plus} and BX_{minus} soils. The used soil batch is indicated at the bottom of the graph. P values of two-sided student's t-tests and replicate numbers are indicated with the boxplots. **(b)** Percent of germinated seeds on ½ MS plates supplemented with DMSO (control) or increasing amounts of MBOA (dissolved in DMSO) recorded during four days after sowing. The P values on top of each time point represent the ANOVA statistics testing for differences between the groups. **(c)** Shoot fresh weight of Arabidopsis plants grown on ½ MS plates supplemented with DMSO (Control) or increasing amounts of MBOA (dissolved in DMSO). One data point represents the total shoot fresh weight from five plants grown on one plate. The P values on top of the boxplots represent the t-test comparison between the Control and the respective MBOA concentration.

the course of the experiment in the non-sterile growth chamber. The detailed microbiota analysis is documented in the **Supplementary Dataset S1**. For bacteria, ordination analysis revealed a clear separation of the communities between soil and between the two groups of roots with strongly differing communities from roots grown in native or initially sterilized soils (**Fig. 3a**). Quantifying the effect sizes of BX-conditioning based on the R^2 values of Permutational Multivariate Analysis of Variance (PERMANOVA), we found significantly different bacterial communities between BX_{minus} and BX_{plus} in all sample groups. BX-conditioning explained 12.2% of the bacterial community variation in soil, 7.3% on roots from native soils and 6.3% on roots from sterilized soils (**Fig. 3a**). We also detected 28 bacterial ASVs in soil and 12 bacterial ASVs on roots from native soil whose abundance was BX-conditioning dependent (**Tables S3, S4**). For the fungi, soil and root communities were separated, but the separation between roots from native and roots from sterilized soil was less marked as for the bacteria (**Fig. 3b**). The fungal communities only differed on roots from sterilized soil, where the BX-conditioning explained 11.7% of the fungal community variation (**Fig. 3b**). Together with the plant growth data (**Fig. 2a**), these experiments suggested that BXs in soil cause a differentiation of the root microbiotas and that these differential microbiotas – particularly the bacteria – would drive the differential growth of Arabidopsis.

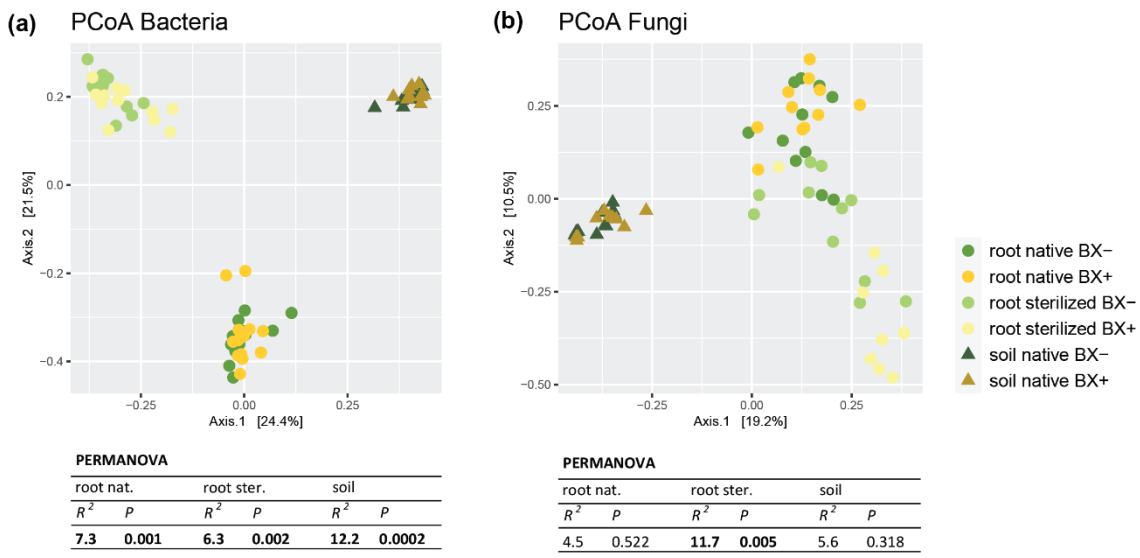

PERMANOVA

root nat.		root ster.		soil	
R^2	P	R^2	P	R^2	P
7.3	**0.001**	**6.3**	**0.002**	**12.2**	**0.0002**

PERMANOVA

root nat.		root ster.		soil	
R^2	P	R^2	P	R^2	P
4.5	0.522	**11.7**	**0.005**	5.6	0.318

Figure 3 The Microbiota of soil and Arabidopsis roots is differentiated by BX-conditioning. Principle Coordinate Analysis (PCoA) of **(a)** bacterial and **(b)** fungal community profiles from native BX_{plus} and BX_{minus} soils, from Arabidopsis roots grown in native BX_{plus} and BX_{minus} soil and from roots grown in initially sterilized BX_{plus} and BX_{minus} soils. The tables below report the PERMANOVA on Bray-Curtis dissimilarities between the three sample groups with R^2 and P values displayed for the conditioning variable. Statistically significant differences are shown in bold. Replicate numbers are n = 10 to 14 for bacterial and n = 9 to 11 for fungal samples.

The shoot transcriptome suggested better defense when Arabidopsis is grown on BX_{plus} soil

To obtain insights into how Arabidopsis achieves better growth on BX_{plus} soil, we performed a transcriptome analysis of shoot and root samples from plants grown for seven weeks on BX_{minus} and BX_{plus} soils (**Fig. S1c**). The detailed RNAseq analysis is documented in the **Supplementary Dataset S2**. Comparing plants grown on control BX_{minus} versus BX_{plus} soil, we found 1959 and 1839 differentially expressed genes (adjusted P value, $P_{adj} < 0.05$; log2 fold change, log2FC > ±1) in shoots (**Table S5**) and roots (**Table S6**), respectively. The subsequent co-expression and gene ontology (GO) enrichment analysis ($P_{adj} < 0.01$; log2FC > ±1) revealed that soil conditioning affected diverse biological processes, both in shoots (**Fig. S3a**, **Table S7**) and roots (**Fig. S3b**, **Table S8**). Because many enriched GO terms were supported by rather few genes, we focused on the top two in each co-expression cluster.

In shoots, 534 genes were upregulated and 1425 were downregulated on BX_{plus} soil compared to the control BX_{minus} soil (**Fig. 4a**, **Table S5**). The main upregulated biological processes involved systemic acquired resistance (SAR), processes of leaf senescence and chlorophyll and protein catabolism as well as response to abscisic acid (**Fig. 4b**, see **Table S7** for GO term numbers). Genes that fall into these GO categories include for instance the abscisic acid response genes NFYA5 and AKS1 or the defense marker genes PR5 and PR2 (**Table S9**; documents also the full names of the gene abbreviations). We also noted that PR1, the classical marker gene for salicylic acid defenses and SAR

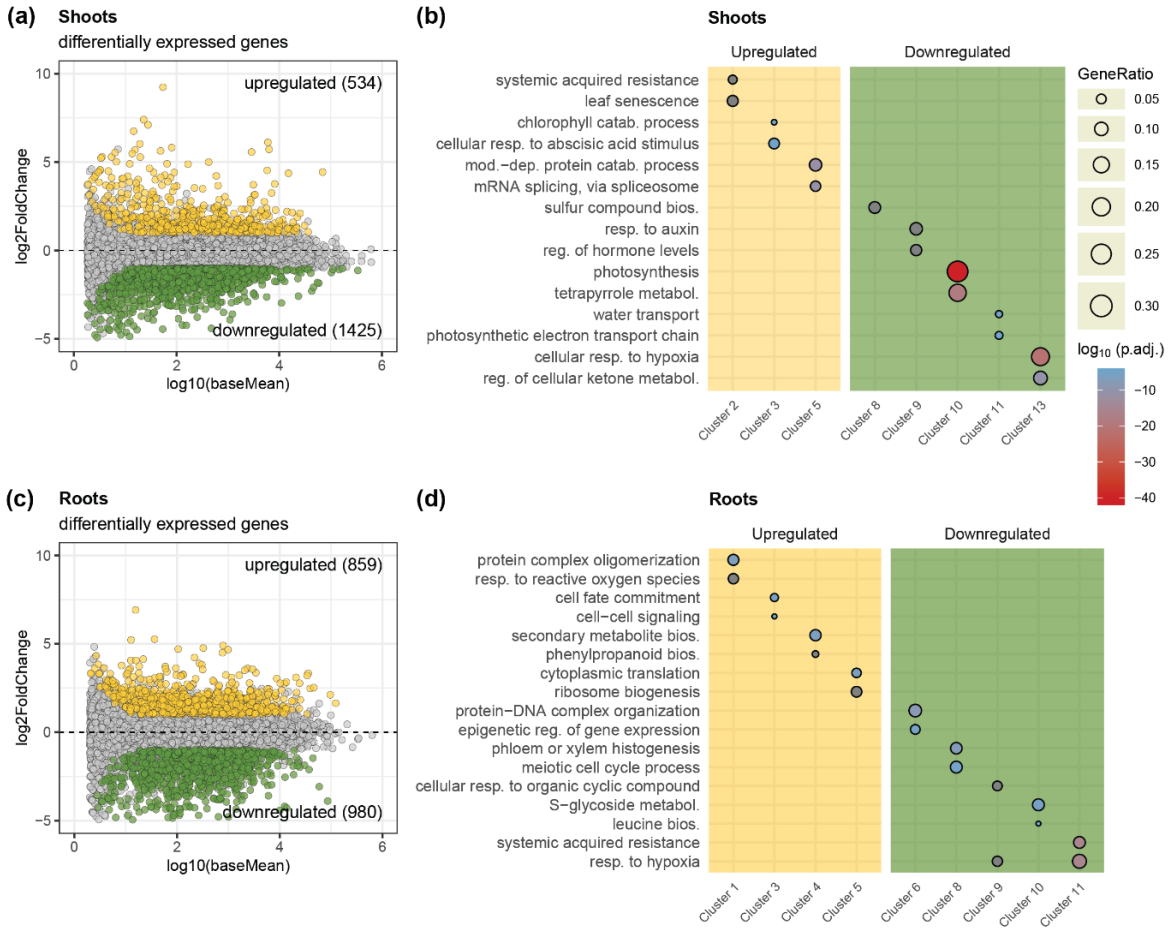

Figure 4 Transcriptome analysis of roots and shoots of Arabidopsis grown on BX_{plus} compared to BX_{minus} soil. (a) MA plot of genes expressed in shoots, plotted by their expression on the x-axis and by the log2FoldChange (log2FC) in expression between BX_{plus} and BX_{minus} soils on the y-axis. Dots in yellow represent genes that were upregulated in shoots grown on BX_{plus} soil compared to BX_{minus} soil ($P_{adj} < 0.05$, log2FC > 1), while green dots represent downregulated genes ($P_{adj} < 0.05$, log2FC < -1), and grey dots represent genes that were not differentially regulated. The total number of differentially expressed genes is reported in the MA plot. **(b)** Representation of the top two GO terms in each co-expression cluster for up- and downregulated genes. The top GO terms per cluster were defined by the highest gene ratios, i.e. fraction of differentially expressed genes of a GO term. Color and size represent the adjusted P values for enrichment of the GO term and its gene ratio, respectively. Some GO terms were shortened due to space (see **Tables S7** and **S8** for full GO terms). **(c)** and **(d)** report the same information for the roots.

(Ryals *et al.*, 1996; van Loon *et al.*, 2006), was significantly up-regulated ($P_{adj} = 0.011$; log2FC = 2.3; **Table S5**).

Downregulated processes in shoots included primarily photosynthesis, metabolization of tetrapyrroles, genes related to decreased oxygen and hypoxia (**Fig. 4b**, **Table S7**). These GO categories were supported with genes like LHCB6, RBCS1A, and CHLI2 involved in photosynthesis and chlorophyll biosynthesis and the hypoxia- and defense related resistance TIR-NBS-LRR proteins TN8 and TN9. Additionally, responses to auxin were also downregulated, including genes like TAA1 and LAX 3 (**Table S9**). Taken together, the shoot transcriptomes revealed that plants growing on BX_{plus} soil

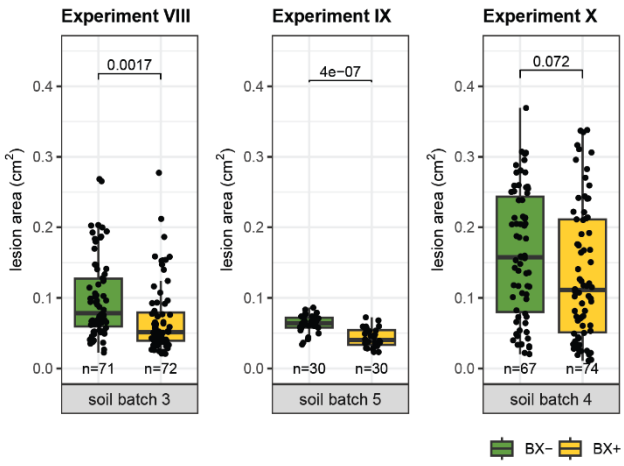

Figure 5 Arabidopsis defense against *Botrytis* was improved on BX_{plus} soil. Quantification of *Botrytis cinerea* infections based on the area of necrotic lesions in cm^2 on Arabidopsis leaves. Plant leaves were infected at five weeks for Experiment IX and at six weeks for experiments VIII and X. P values of two-sided student's t-tests are displayed above each comparison and sample sizes are indicated at the bottom of each boxplot. The soil batch is indicated at the bottom of the graphs.

were developmentally more advanced, i.e. towards senescence and with reduced photosynthesis, while having activated defenses.

In roots, 859 and 980 genes were up- or downregulated, respectively (**Fig. 4c**, **Table S6**). The main upregulated biological processes included protein complex oligomerization, response to reactive oxygen species, cell fate commitment and signaling, and secondary metabolite biosynthesis in general with the phenylpropanoid pathway in particular (**Fig. 4d**, **Table S8**). Genes of these GO categories included for instance MYB66/WER and MYB23 involved in root epidermis determination and cell differentiation, PRR1 and MYB43 for lignin biosynthesis and the sugar transporters SWEET4 and SWEET12 (**Table S9**). The main downregulated processes in roots were related to systemic acquired resistance, responses to low oxygen, S-glycoside metabolism and developmental processes like cell cycle, tissue generation and gene regulation (**Fig. 4b**, **Table S8**). Support for these GO categories included the defense related genes MKK7, WRKY40, CRK9 and the receptors TN7 and TN8 (**Table S9**). However, this difference in expression seems to be mainly driven by two BX_{minus} samples with very high expressions (cluster 11, **Fig. S3b)**. We also noticed the glucosinolate biosynthesis to be downregulated (cluster 10, **Fig. S3b**, **Table S8**), particularly with the genes FMO GS-OX1 and IMD1 related to aliphatic compounds (**Table S9**). In summary, the root transcriptomes revealed that plants growing on BX_{plus} soil alter root developmental processes and have downregulated defenses. Overall, we concluded that BX-conditioning changes defense processes in both shoots and roots, and also alters growth related processes such as photosynthesis.

Arabidopsis grown on BX_{plus} soil was better defended against *Botrytis*

The transcriptome analysis revealed a signature of enhanced defenses in shoots of plants grown on BX_{plus} soil (**Fig. 4**). To compare the defense responses of Arabidopsis on BX_{plus} soil compared to BX_{minus} soil, we infected leaves with the necrotrophic fungus *Botrytis cinerea* and quantified the area of the developing lesions. We recorded smaller lesions on plants grown on BX_{plus} compared to BX_{minus} soil in three independent experiments performed on three different soil batches (**Fig. 5**). These results indicate that Arabidopsis is more resistant to *B. cinerea* when grown on BX_{plus} compared to BX_{minus} soil, which confirmed the signature for enhanced defenses in shoots of plants grown on BX_{plus} soil.

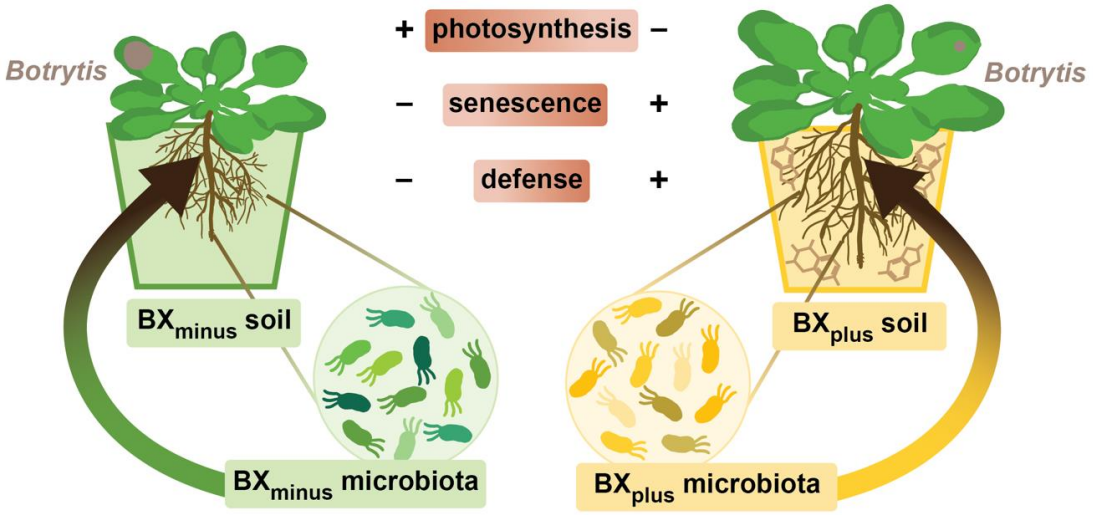

Figure 6 BX-feedbacks in Arabidopsis affect growth and defense. Model for feedbacks on Arabidopsis when plants are grown on BX_{plus} soil compared to the control soil BX_{minus}. BX_{plus} and BX_{minus} soils are physico-chemically the same, but differ in conditioning by the previous plant generation, being either wild-type benzoxazinoid (BX) exuding maize or non BX-exuding mutant lines, respectively. The exudation of BXs to soil (indicated with chemical structures in the BX_{plus} pot) affects the microbiota composition. Arabidopsis grown on BX_{plus} soil shows increased root and shoot growth and is better defended against *Botrytis cinerea* (lesion sizes are indicated) compared to Arabidopsis grown on BX_{minus} soil. These phenotypic feedbacks were supported by shoot transcriptome analyses (brown boxes), which revealed that plants on BX_{plus} soil were developmentally more advanced, with reduced photoynthesis and increased senesence processes, and that they had enhanced defenses. On the roots of Arabidopsis, we found differential bacterial communities, which we call BX_{minus} and BX_{plus} microbiota respectively. As the positive growth on BX_{plus} soil was lost after soil sterilization, we propose that the differential microbiotas shape these growth feedbacks, depicted by the arrows leading from the microbiota back to the plant.

Discussion

Plant soil feedbacks (PSFs) describe the performance of a new plant generation to the soil legacy caused by the previous plant generation. We previously established a system to study PSFs where maize growth leads to BX-dependent alterations of the soil microbiota, which then drives the feedbacks of next generation maize or wheat plants (Hu *et al.*, 2018; Cadot *et al.*, 2021). Mechanistically, how plants respond to altered soil microbiotas and in turn modulate their own performance is not well understood so far. In this study, we employed Arabidopsis to investigate its feedback responses to differential microbiotas in soil, which were established by differential BX exudation of maize. Below, we summarize our results and discuss the implications of our findings in the context of BX-feedbacks, and in a broader context of how plants mediate microbiome feedbacks.

Arabidopsis as a model to study microbiome feedbacks

We found that Arabidopsis responded with increased shoot and root growth and also enhanced resistance to shoot infections with the pathogen *Botrytis cinerea* when grown on BX_{plus} soil (**Fig. 6**). These BX-feedback phenotypes were consistent with the transcriptome analysis revealing that plants were developmentally more advanced (earlier senescence, reduced photosynthesis) while having enhanced defenses in shoots when grown on BX_{plus} soil. We found differential root microbiotas when Arabidopsis was grown on the two soils and also that the positive growth feedback was lost after soil sterilization. This is consistent with earlier work on maize, where the differential soil microbiotas and the loss of feedback after sterilization lead to the conclusion that the feedbacks were dependent on BXs but mediated by soil microbes (Hu *et al.*, 2018). This suggests that soil microbes also drive the observed BX-feedback phenotypes in Arabidopsis. Thus, the occurrence of microbially driven BX-feedbacks and the many available research resources make Arabidopsis a good model to study the molecular mechanisms of BX-feedbacks.

Direction of feedback responses

The Arabidopsis Col-0 accession tested here responded with enhanced growth on BX_{plus} compared to BX_{minus} soil, which is a positive BX-feedback (**Fig. 1**). This is in contrast to maize, where the two inbreed lines W22 and B73 had equal or reduced shoot biomasses, respectively, on BX_{plus} compared to BX_{minus} soil (Hu *et al.*, 2018; Cadot *et al.*, 2021; Gfeller *et al.*, 2023a). Thus, we find neutral or negative growth feedbacks with maize. When we previously tested different wheat varieties in different soils, we found more inconsistencies in the directions of BX-feedbacks – from positive to neutral to negative. Negative shoot biomass feedbacks were recorded for the wheat varieties Claro on ‘Changins’ soil (Gfeller *et al.*, 2023a) and for Drifter and Fiorina in ‘Changins’ and ‘Reckenholz’ soils (Cadot *et al.*, 2021), while we measured positive biomass feedbacks for Sailor, Claro and Fiorina but on ‘Posieux’ soil (Gfeller *et al.*, 2023b). These observations suggest that the varying feedback direction – positive or negative – depends both on the soil environment and on the genotype of the response plant. For the

former, we have demonstrated that BX-feedbacks can vary in strength and direction along a chemical gradient that exists within a tested field in Changins (Gfeller *et al.*, 2023a). Future work is needed to extend on the second part of the above conclusion - whether and how the genotype of the response plant influences the direction of BX-feedbacks. Arabidopsis with its many accessions might be useful in uncovering genetic components of such microbiome feedbacks.

Microbiome or chemical feedbacks?

The finding that the better growth of Arabidopsis on native BX_{plus} soil is reversed on sterilized soils (**Fig. 2a**) requires a detailed reflection. While the soil microbiota is eliminated by initial soil sterilization, the BX concentrations stay intact (**Fig. S2a**) and represent the main chemical difference between BX_{minus} and BX_{plus} soil, as classical chemical soil properties like macro- and micronutrients, soil composition or pH do not differ (Hu *et al.*, 2018; Gfeller *et al.*, 2023b). The feedbacks on plants could thus be mediated not only by a microbial but also chemical BX component. Arabidopsis growth could be directly affected by BXs in soil, as AMPO (Venturelli *et al.*, 2015) and MBOA (**Fig. 2bc**) can have direct inhibitory activity on Arabidopsis growth when tested in vitro. However, effective concentrations in vitro were much higher, and even the lowest non-inhibitory concentrations that were tested in vitro were four (MBOA; this study) and three (AMPO; Venturelli *et al.*, 2015) orders of magnitude higher than the concentrations that we measured in soil (**Fig. S2a**). Yet in soil, Arabidopsis is exposed to both metabolites simultaneously, which could still lead to a direct inhibitory effect on growth.

However, such a chemical component in BX-feedbacks only became apparent in sterilized soil in absence of a native BX_{plus} microbiota, as Arabidopsis grew better on native BX_{plus} soil compared to native BX_{minus} soil. This suggests that chemical and allelopathic effects were masked by the growth promoting activities of the BX_{plus} microbiota. Additionally, the observation of differentiated microbiotas on roots grown in sterilized soils (**Fig. 3ab**) suggests that the residual BXs in sterilized soils were driving these microbiota differences, which then could have led to the reduction in plant growth on sterilized BX_{plus} soil. Therefore, we concluded that the chemical component of BX-feedbacks with Arabidopsis plays a more indirect role, and that BX-feedbacks are primarily driven through interactions with the soil microbiota that then affect plant growth.

Developmental advance of BX_{plus} grown plants

We have performed a transcriptome analysis to investigate how Arabidopsis achieves the better growth on BX_{plus} soil. While no typical growth-related processes were upregulated, we found that photosynthesis related genes were downregulated and senescence processes upregulated in plants grown on BX_{plus} soil (**Fig. 4**). Together, this suggested that the larger rosettes of the plants on BX_{plus} soil were because these plants were developmentally more advanced compared to the plants grown on BX_{minus} soil. The gene expression analysis revealed, ahead of time and without showing signs of

senescence in plants, that the bigger plants on BX_{plus} soil might have reached the end of their vegetative growth phase. This is also consistent with the late sampling timepoint of seven-week-old plants. A possible explanation for the developmental advance could be differences in germination, as previous work with wheat showed better germination on BX_{plus} compared to BX_{minus} soil (Gfeller *et al.*, 2023b). This earlier germination had provided the wheat plants a big enough head start to the growth period, leading to higher tiller densities and enhanced biomass at harvest. Future experiments are needed to clarify if germination effects or other early developmental processes are also involved in BX-feedbacks with Arabidopsis.

BX_{plus} grown plants have enhanced defenses

Previously, we have reported better resistance of maize against herbivores when grown on BX_{plus} compared to BX_{minus} soil (Hu *et al.*, 2018; Cadot *et al.*, 2021). In this study, we found increased resistance of Arabidopsis against the necrotrophic pathogen *Botrytis cinerea* when grown on BX_{plus} soil (**Fig. 5**). In maize, this better defense coincided with higher levels of the defense hormones salicylic acid (SA) and jasmonic acid (JA), as well as increased expression of JA-related defense marker genes in the shoots, even when plants were unchallenged (Hu *et al.*, 2018). Thus, increased JA-related defense markers on BX_{plus} soil might have facilitated resistance against caterpillars, as defense against herbivores and necrotrophic pathogens mainly requires the JA-related defense pathway (Shigenaga & Argueso, 2016).

In Arabidopsis however, we found SA-dependent defenses to be upregulated in the shoots of Arabidopsis grown on BX_{plus} soil, as evidenced with the increased expression of typical SA-dependent marker genes including PR1, PR2 and PR5 (**Fig. 4**). Nevertheless, PR genes are also upregulated during *B. cinerea* infection (Govrin & Levine, 2002), therefore higher PR expression levels on BX_{plus} soil could still mediate the increased resistance of Arabidopsis to *B. cinerea*. Future work should clarify whether Arabidopsis could also benefit from enhanced resistance against other pathogens on BX_{plus} soil.

The BX_{plus} microbiota primes for enhanced defenses?

Due to limited resources, plants constantly face the dilemma of where to invest, into growth or defense; this dilemma is known as the growth-defense trade-off (He *et al.*, 2022). For the growth of Arabidopsis plants on BX_{plus} soil, we found both increased growth (**Fig. 1**) and enhanced defense (**Fig. 5**), which is not in agreement with a classical growth-defense trade-off. One possible explanation could be that the enhanced resistance is not explained by a plant trait itself, but that it is a consequence of for example antagonistic effects of the leaf microbiota, which we did not analyse in this study. Recently, it was shown that the growth of Arabidopsis plants infected with the downy mildew *Hyaloperonospora arabidopsidis* (HPA) enriches the soil for a set of disease suppressive bacteria, which then also colonize the leaves of the feedback plant and reduce the sporulation of HPA directly on the leaf (Goossens *et al.*,

2023). Therefore, direct microbe-microbe interactions on the leaves could be responsible for the enhanced resistance against *Botrytis cinerea* on BX_{plus} soil.

Another possible explanation is that plants on BX_{plus} soil only induce an enhanced defense response compared to plants on BX_{minus} soil when they are infected with *Botrytis cinerea*. As plants were grown in climate chambers in absence of constant pathogen or pest pressure, they likely did not need to invest in costly constitutive defenses. Instead, we hypothesize that the plants on BX_{plus} soil are primed for inducible defenses, which usually does not impair growth. Priming is a state of alert where upon a pathogen or pest attack, plants can mount a faster and stronger defense response than un-primed plants (Martinez-Medina *et al.*, 2016; Karasov *et al.*, 2017; Harris *et al.*, 2023). The state of priming is established by a preceding priming stimulus, such as a defended pathogen attack which is described as systemic acquired resistance (SAR; Ross, 1961; Zeier, 2021), or root colonization by beneficial microbes, which is known as induced systemic resistance (ISR; Pieterse *et al.*, 1996, 2014).

ISR and SAR are typically studied with single beneficial or pathogenic strains, but there is emerging evidence that also whole soil microbiotas can elicit ISR to enhance resistance for example against herbivores (Badri *et al.*, 2013; Hubbard *et al.*, 2019; Pineda *et al.*, 2020). Hence, it appears plausible that priming via ISR or SAR, or even via both processes, can occur in complex microbiotas as it is the case with the differential BX_{plus} and BX_{minus} microbiotas used in our study. Future experiments are needed to test if and via which mechanism Arabidopsis is primed when growing on BX_{plus} soil. Collectively, priming could serve as an explanatory mechanism for the lack of a growth-defense trade-off, which was observed with the improved growth and the enhanced resistance of Arabidopsis on BX_{plus} soil.

Conclusion

The potential to utilize the beneficial functions of the root microbiome as a more sustainable way to improve plant growth and health in agriculture is well recognized (French *et al.*, 2021; Santos & Olivares, 2021). However, the mechanisms by which plants perceive and respond to specific soil microbiomes are currently not well understood (Janse van Rensburg *et al.*, 2024). Our study provides a first step into this direction, as we show that Arabidopsis can respond with both improved growth and enhanced resistance on a specific soil microbiota. The model system of BX-feedbacks on Arabidopsis will allow us to further study the mechanisms by which Arabidopsis can perceive and mediate microbiome feedbacks, and especially to identify the plant genes that are important for this process. Possibly, such knowledge can help to improve breeding programs so that crops can take full advantage of their microbiome.

Acknowledgements

We sincerely thank Nicolas Widmer (Agroscope Changins, Switzerland) for field access and assistance in soil sampling, Prof. Tobias Züst (University of Zurich, Switzerland) and Mirco Hecht (Federal Statistical Office, Switzerland) for the BX analysis, and Dr. Phillipe Demougin and Dr. Geoffrey Fucile (both University of Basel, Switzerland) for preparation and sequencing of the RNAseq library. Furthermore, we thank Corinne Suter (University of Bern, Switzerland) for implementing the 'in vitro Experiment I', Markus Funk (University of Basel, Switzerland) for performing the RNA extractions, Dr. Selma Cadot (Agroscope Reckenholz, Switzerland) for collecting field soil, Jan Wälchli (University of Basel, Switzerland) for assembling the microbiota reads and Florian Enz (University of Bern, Switzerland) for maintaining the maize plants. Lastly, we are also grateful to Prof. Christelle Robert and Prof. Matthias Erb (both University of Bern, Switzerland) for providing the maize seeds, and to Prof. Wim Van den Ende (KU Leuven, Belgium) for providing us with the *Botrytis cinerea* strain. This work was mainly supported by funding of the University of Basel and partly by the Swiss National Science Foundation (No. 189249 to K.S.).

Competing interests

The authors declare not to hold a conflict of interest or competing interests.

Author contributions

KSt, LT and KS planned and designed the research. KSt, HJvR, LT and VD performed experiments. KSt and LS analysed the data. KSt and KS wrote the manuscript.

Data availability

The source data on plant biomass and soil physicochemical analyses is made publicly available on https://github.com/PMI-Basel/Stengele_et_al_At_BX-feedbacks. The raw sequencing data are stored at the European Nucleotide Archive (http://www.ebi.ac.uk/ena). The RNA Seq sequencing data is stored under project number PRJEB80860, and the microbiota sequencing data is available under the project number PRJEB59165 (The 16S rRNA and ITS gene libraries of this study were sequenced in the same MiSeq run together with a library of an already published project (Gfeller *et al.*, 2023a)). The bioinformatic code including information on barcodes, primers and sample assignments is provided on GitHub. On GitHub we have also deposited all code used for statistical analysis and graphing of all figures.

References

Abarenkov K, Nilsson RH, Larsson K-H, Taylor AFS, May TW, Frøslev TG, Pawlowska J, Lindahl B, Põldmaa K, Truong C, *et al.* 2024. The UNITE database for molecular identification and taxonomic communication of fungi and other eukaryotes: sequences, taxa and classifications reconsidered. *Nucleic Acids Research* **52**: D791–D797.

Badri DV, Zolla G, Bakker MG, Manter DK, Vivanco JM. **2013**. Potential impact of soil microbiomes on the leaf metabolome and on herbivore feeding behavior. *New Phytologist* **198**: 264–273.

Bai B, Liu W, Qiu X, Zhang J, Zhang J, Bai Y. **2022**. The root microbiome: Community assembly and its contributions to plant fitness. *Journal of Integrative Plant Biology* **64**: 230–243.

Bezemer TM, Lawson CS, Hedlund K, Edwards AR, Brook AJ, Igual JM, Mortimer SR, Van Der Putten WH. **2006**. Plant species and functional group effects on abiotic and microbial soil properties and plant–soil feedback responses in two grasslands. *Journal of Ecology* **94**: 893–904.

Bray JR, Curtis JT. **1957**. An ordination of the upland forest communities of southern wisconsin. *Ecological Monographs* **27**: 325–349.

Bulgarelli D, Schlaeppi K, Spaepen S, van Themaat EVL, Schulze-Lefert P. **2013**. Structure and functions of the bacterial microbiota of plants. *Annual Review of Plant Biology* **64**: 807–838.

Cadot S, Gfeller V, Hu L, Singh N, Sánchez-Vallet A, Glauser G, Croll D, Erb M, Heijden MGA, Schlaeppi K. **2021**. Soil composition and plant genotype determine benzoxazinoid-mediated plant–soil feedbacks in cereals. *Plant, Cell & Environment* **44**: 3732–3744.

Callahan BJ, McMurdie PJ, Rosen MJ, Han AW, Johnson AJA, Holmes SP. **2016**. DADA2: High-resolution sample inference from Illumina amplicon data. *Nature Methods* **13**: 581–583.

Cardoso C, Charnikhova T, Jamil M, Delaux P-M, Verstappen F, Amini M, Lauressergues D, Ruyter-Spira C, Bouwmeester H. **2014**. Differential activity of Striga hermonthica seed germination stimulants and Gigaspora rosea hyphal branching factors in rice and their contribution to underground communication (M Öpik, Ed.). *PLoS ONE* **9**: e104201.

Cotton TEA, Pétriacq P, Cameron DD, Meselmani MA, Schwarzenbacher R, Rolfe SA, Ton J. **2019**. Metabolic regulation of the maize rhizobiome by benzoxazinoids. *The ISME Journal* **13**: 1647–1658.

Delory BM, Callaway RM, Semchenko M. **2024**. A trait-based framework linking the soil metabolome to plant–soil feedbacks. *New Phytologist* **241**: 1910–1921.

Dobin A, Davis CA, Schlesinger F, Drenkow J, Zaleski C, Jha S, Batut P, Chaisson M, Gingeras TR. **2013**. STAR: ultrafast universal RNA-seq aligner. *Bioinformatics* **29**: 15–21.

Durán P, Thiergart T, Garrido-Oter R, Agler M, Kemen E, Schulze-Lefert P, Hacquard S. **2018**. Microbial interkingdom interactions in roots promote Arabidopsis survival. *Cell* **175**: 973-983.e14.

Fernandes AD, Macklaim JM, Linn TG, Reid G, Gloor GB. **2013**. ANOVA-like differential expression (ALDEx) analysis for mixed population RNA-Seq. *PLOS ONE* **8**: e67019.

Fernandes AD, Reid JN, Macklaim JM, McMurrough TA, Edgell DR, Gloor GB. **2014**. Unifying the analysis of high-throughput sequencing datasets: characterizing RNA-seq, 16S rRNA gene sequencing and selective growth experiments by compositional data analysis. *Microbiome* **2**: 15.

French E, Kaplan I, Iyer-Pascuzzi A, Nakatsu CH, Enders L. 2021. Emerging strategies for precision microbiome management in diverse agroecosystems. *Nature Plants* **7**: 256–267.

Gfeller V, Cadot S, Waelchli J, Gulliver S, Terrettaz C, Thönen L, Mateo P, Robert CAM, Mascher F, Steinger T, *et al.* 2023a. Soil chemical and microbial gradients determine accumulation of root-exuded secondary metabolites and plant–soil feedbacks in the field. *Journal of Sustainable Agriculture and Environment*: sae2.12063.

Gfeller V, Waelchli J, Pfister S, Deslandes-Hérold G, Mascher F, Glauser G, Aeby Y, Mestrot A, Robert CA, Schlaeppi K, *et al.* 2023b. Plant secondary metabolite-dependent plant-soil feedbacks can improve crop yield in the field. *eLife* **12**: e84988.

Goossens P, Spooren J, Baremans KCM, Andel A, Lapin D, Echobardo N, Pieterse CMJ, Van Den Ackerveken G, Berendsen RL. 2023. Obligate biotroph downy mildew consistently induces near-identical protective microbiomes in Arabidopsis thaliana. *Nature Microbiology* **8**: 2349–2364.

Govrin EM, Levine A. 2002. Infection of Arabidopsis with a necrotrophic pathogen, Botrytis cinerea, elicits various defense responses but does not induce systemic acquired resistance (SAR). *Plant Molecular Biology* **48**: 267–276.

Harris CJ, Amtmann A, Ton J. 2023. Epigenetic processes in plant stress priming: Open questions and new approaches. *Current Opinion in Plant Biology* **75**: 102432.

He Z, Webster S, He SY. 2022. Growth–defense trade-offs in plants. *Current Biology* **32**: R634–R639.

Hu L, Robert CAM, Cadot S, Zhang X, Ye M, Li B, Manzo D, Chervet N, Steinger T, van der Heijden MGA, *et al.* 2018. Root exudate metabolites drive plant-soil feedbacks on growth and defense by shaping the rhizosphere microbiota. *Nature Communications* **9**: 2738.

Hubbard CJ, Li B, McMinn R, Brock MT, Maignien L, Ewers BE, Kliebenstein D, Weinig C. 2019. The effect of rhizosphere microbes outweighs host plant genetics in reducing insect herbivory. *Molecular Ecology* **28**: 1801–1811.

Hüther P, Schandry N, Jandrasits K, Bezrukov I, Becker C. 2020. ARADEEPOPSIS, an automated workflow for top-view plant phenomics using semantic segmentation of leaf states. *The Plant Cell* **32**: 3674–3688.

Jacoby RP, Koprivova A, Kopriva S. 2021. Pinpointing secondary metabolites that shape the composition and function of the plant microbiome (R Hancock, Ed.). *Journal of Experimental Botany* **72**: 57–69.

Janse van Rensburg H, Stengele K, Schlaeppi K. 2024. Understanding plant responsiveness to microbiome feedbacks. *Current Opinion in Plant Biology* **81**: 102603.

Jing J, Cong W-F, Bezemer TM. 2022. Legacies at work: plant–soil–microbiome interactions underpinning agricultural sustainability. *Trends in Plant Science* **27**: 781–792.

Karasov TL, Chae E, Herman JJ, Bergelson J. 2017. Mechanisms to mitigate the trade-off between growth and defense. *The Plant Cell* **29**: 666–680.

Korenblum E, Massalha H, Aharoni A. 2022. Plant–microbe interactions in the rhizosphere via a circular metabolic economy. *The Plant Cell* **34**: 3168–3182.

Kudjordjie EN, Sapkota R, Steffensen SK, Fomsgaard IS, Nicolaisen M. **2019**. Maize synthesized benzoxazinoids affect the host associated microbiome. *Microbiome* **7**: 59.

Lin H, Peddada SD. **2020**. Analysis of compositions of microbiomes with bias correction. *Nature Communications* **11**: 3514.

Lindsey III BE, Rivero L, Calhoun CS, Grotewold E, Brkljacic J. **2017**. Standardized method for high-throughput sterilization of Arabidopsis seeds. *Journal of Visualized Experiments*: 56587.

van Loon LC, Rep M, Pieterse CMJ. **2006**. Significance of inducible defense-related proteins in infected plants. *Annual Review of Phytopathology* **44**: 135–162.

Love MI, Huber W, Anders S. **2014**. Moderated estimation of fold change and dispersion for RNA-seq data with DESeq2. *Genome biology* **15**: 1–21.

Maag D, Köhler A, Robert CAM, Frey M, Wolfender J-L, Turlings TCJ, Glauser G, Erb M. **2016**. Highly localized and persistent induction of Bx1-dependent herbivore resistance factors in maize. *The Plant Journal* **88**: 976–991.

Mariotte P, Mehrabi Z, Bezemer TM, De Deyn GB, Kulmatiski A, Drigo B, Veen GF (Ciska), van der Heijden MGA, Kardol P. **2018**. Plant–soil feedback: Bridging natural and agricultural sciences. *Trends in Ecology & Evolution* **33**: 129–142.

Martin M. **2011**. Cutadapt removes adapter sequences from high-throughput sequencing reads. *EMBnet.journal* **17**: 10–12.

Martinez-Medina A, Flors V, Heil M, Mauch-Mani B, Pieterse CMJ, Pozo MJ, Ton J, van Dam NM, Conrath U. **2016**. Recognizing plant defense priming. *Trends in Plant Science* **21**: 818–822.

McMurdie PJ, Holmes S. **2013**. phyloseq: An R package for reproducible interactive analysis and graphics of microbiome census data. *PLOS ONE* **8**: e61217.

Niculaes C, Abramov A, Hannemann L, Frey M. **2018**. Plant protection by Benzoxazinoids—recent insights into biosynthesis and function. *Agronomy* **8**: 143.

Niemeyer HM. **2009**. Hydroxamic acids derived from 2-Hydroxy-2 *H* -1,4-Benzoxazin-3(4 *H*)-one: Key defense chemicals of cereals. *Journal of Agricultural and Food Chemistry* **57**: 1677–1696.

Paulson JN, Stine OC, Bravo HC, Pop M. **2013**. Differential abundance analysis for microbial marker-gene surveys. *Nature Methods* **10**: 1200–1202.

Pieterse CMJ, Van Wees SCM, Hoffland, Ellis, Van Pelt JA, Loon LC van. **1996**. Systemic resistance in Arabidopsis induced by biocontrol bacteria is independent of salicylic acid accumulation and pathogenesis-related gene expression. *The Plant Cell* **8**: 1225–1237.

Pieterse CMJ, Zamioudis C, Berendsen RL, Weller DM, Van Wees SCM, Bakker PAHM. **2014**. Induced systemic resistance by beneficial microbes. *Annual Review of Phytopathology* **52**: 347–375.

Pineda A, Kaplan I, Hannula SE, Ghanem W, Bezemer TM. **2020**. Conditioning the soil microbiome through plant–soil feedbacks suppresses an aboveground insect pest. *New Phytologist* **226**: 595–608.

Posit team. **2023**. *RStudio: Integrated Development Environment for R*. Boston, MA: Posit Software, PBC.

van der Putten WH, Bardgett RD, Bever JD, Bezemer TM, Casper BB, Fukami T, Kardol P, Klironomos JN, Kulmatiski A, Schweitzer JA, *et al.* 2013. Plant–soil feedbacks: the past, the present and future challenges. *Journal of Ecology* **101**: 265–276.

Quast C, Pruesse E, Yilmaz P, Gerken J, Schweer T, Yarza P, Peplies J, Glöckner FO. **2013**. The SILVA ribosomal RNA gene database project: improved data processing and web-based tools. *Nucleic Acids Research* **41**: D590–D596.

R Core Team. **2017**. *R: A language and environment for statistical computing*. Vienna, Austria: R Foundation for Statistical Computing.

Rau A, Maugis-Rabusseau C. **2018**. Transformation and model choice for RNA-seq co-expression analysis. *Briefings in bioinformatics* **19**: 425–436.

Robert CAM, Mateo P. **2022**. The chemical ecology of Benzoxazinoids. *CHIMIA* **76**: 928.

Ross AF. **1961**. Systemic acquired resistance induced by localized virus infections in plants. *Virology* **14**: 340–358.

Ryals JA, Neuenschwander UH, Willits MG, Molina A, Steiner H-Y, Hunt MD. **1996**. Systemic acquired resistance. *The Plant Cell* **8**: 1809–1819.

Salas-González I, Reyt G, Flis P, Custódio V, Gopaulchan D, Bakhoum N, Dew TP, Suresh K, Franke RB, Dangl JL, *et al.* 2021. Coordination between microbiota and root endodermis supports plant mineral nutrient homeostasis. *Science* **371**: eabd0695.

Santos LF, Olivares FL. **2021**. Plant microbiome structure and benefits for sustainable agriculture. *Current Plant Biology* **26**: 100198.

Sasse J, Martinoia E, Northen T. **2018**. Feed your friends: Do plant exudates shape the root microbiome? *Trends in Plant Science* **23**: 25–41.

Schandry N, Becker C. **2020**. Allelopathic plants: Models for studying plant–interkingdom interactions. *Trends in Plant Science* **25**: 176–185.

Schindelin J, Arganda-Carreras I, Frise E, Kaynig V, Longair M, Pietzsch T, Preibisch S, Rueden C, Saalfeld S, Schmid B, *et al.* 2012. Fiji: an open-source platform for biological-image analysis. *Nature Methods* **9**: 676–682.

Schmitz L, Yan Z, Schneijderberg M, de Roij M, Pijnenburg R, Zheng Q, Franken C, Dechesne A, Trindade LM, van Velzen R, *et al.* 2022. Synthetic bacterial community derived from a desert rhizosphere confers salt stress resilience to tomato in the presence of a soil microbiome. *The ISME Journal* **16**: 1907–1920.

Schneider CA, Rasband WS, Eliceiri KW. **2012**. NIH Image to ImageJ: 25 years of image analysis. *Nature Methods* **9**: 671–675.

Semchenko M, Barry KE, Vries FT, Mommer L, Moora M, Maciá-Vicente JG. **2022**. Deciphering the role of specialist and generalist plant–microbial interactions as drivers of plant–soil feedback. *New Phytologist* **234**: 1929–1944.

Shigenaga AM, Argueso CT. **2016**. No hormone to rule them all: Interactions of plant hormones during the responses of plants to pathogens. *Seminars in Cell & Developmental Biology* **56**: 174–189.

Spooren J, Van Bentum S, Thomashow LS, Pieterse CMJ, Weller DM, Berendsen RL. **2024**. Plant-driven assembly of disease-suppressive soil microbiomes. *Annual Review of Phytopathology* **62**: 1–30.

Stringlis IA, Yu K, Feussner K, de Jonge R, Van Bentum S, Van Verk MC, Berendsen RL, Bakker PAHM, Feussner I, Pieterse CMJ. **2018**. MYB72-dependent coumarin exudation shapes root microbiome assembly to promote plant health. *Proceedings of the National Academy of Sciences* **115**.

Teasdale JR, Rice CP, Cai G, Mangum RW. **2012**. Expression of allelopathy in the soil environment: soil concentration and activity of benzoxazinoid compounds released by rye cover crop residue. *Plant Ecology* **213**: 1893–1905.

Trivedi P, Leach JE, Tringe SG, Sa T, Singh BK. **2020**. Plant–microbiome interactions: from community assembly to plant health. *Nature Reviews Microbiology* **18**: 607–621.

Venturelli S, Belz RG, Kämper A, Berger A, Von Horn K, Wegner A, Böcker A, Zabulon G, Langenecker T, Kohlbacher O, *et al.* 2015. Plants release precursors of histone deacetylase inhibitors to suppress growth of competitors. *The Plant Cell* **27**: 3175–3189.

Venturelli S, Petersen S, Langenecker T, Weigel D, Lauer UM, Becker C. **2016**. Allelochemicals of the phenoxazinone class act at physiologically relevant concentrations. *Plant Signaling & Behavior* **11**: e1176818.

Weiss SJ, Xu Z, Amir A, Peddada S, Bittinger K, Gonzalez A, Lozupone C, Zaneveld JR, Vazquez-Baeza Y, Birmingham A, *et al.* 2015. Effects of library size variance, sparsity, and compositionality on the analysis of microbiome data.

Wouters FC, Blanchette B, Gershenzon J, Vassão DG. **2016**. Plant defense and herbivore counter-defense: benzoxazinoids and insect herbivores. *Phytochemistry Reviews* **15**: 1127–1151.

Wu T, Hu E, Xu S, Chen M, Guo P, Dai Z, Feng T, Zhou L, Tang W, Zhan L, *et al.* 2021. clusterProfiler 4.0: A universal enrichment tool for interpreting omics data. *Innovation (Cambridge (Mass.))* **2**: 100141.

Yu P, He X, Baer M, Beirinckx S, Tian T, Moya YAT, Zhang X, Deichmann M, Frey FP, Bresgen V, *et al.* 2021. Plant flavones enrich rhizosphere Oxalobacteraceae to improve maize performance under nitrogen deprivation. *Nature Plants* **7**: 481–499.

Zeier J. **2021**. Metabolic regulation of systemic acquired resistance. *Current Opinion in Plant Biology* **62**: 102050.

Supplementary Information

Benzoxazinoid-mediated microbiome feedbacks enhance Arabidopsis growth and defense

Katja Stengele, Lea Stauber, Lisa Thoenen, Henry Janse van Rensburg, Viola D'Adda, Klaus Schlaeppi

Index

- Supplementary Figures
- Supplementary Tables
- Supplementary Datasets

Supplementary Figures

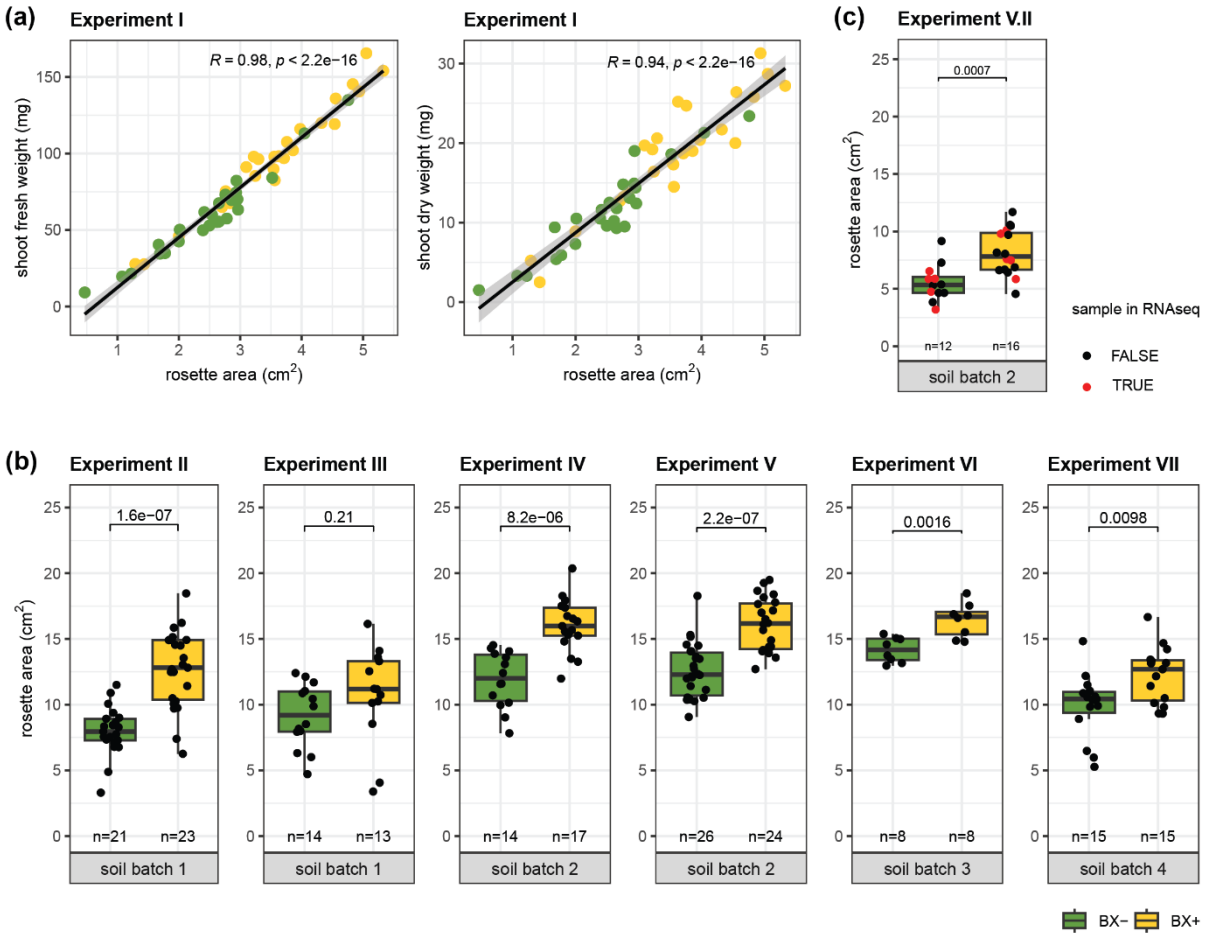

Figure S1 Arabidopsis shoot measurement correlations and growth on different soil batches. (a) Correlation of Arabidopsis rosette area to shoot biomass (shoot fresh weight and shoot dry weight). The pearson correlation coefficient and respective P value for the correlation are displayed within the graph. **(b)** Arabidopsis rosette area from six independent experiments. Note that the shoot area data for Experiment III are also shown in Fig. 2a. The soil batch number, indicated at the bottom of each individual plot, denotes the independent conditioning events of the soil by growing maize. **(c)** Rosette area from the experiment where plant material was harvested for the RNASeq analysis. The red dots indicate the plant replicates where the shoot and root transcriptome had been sequenced for the RNASeq analysis. In (b) and (c), boxplots report the P values of two-sided student's t-tests and the replicate numbers.

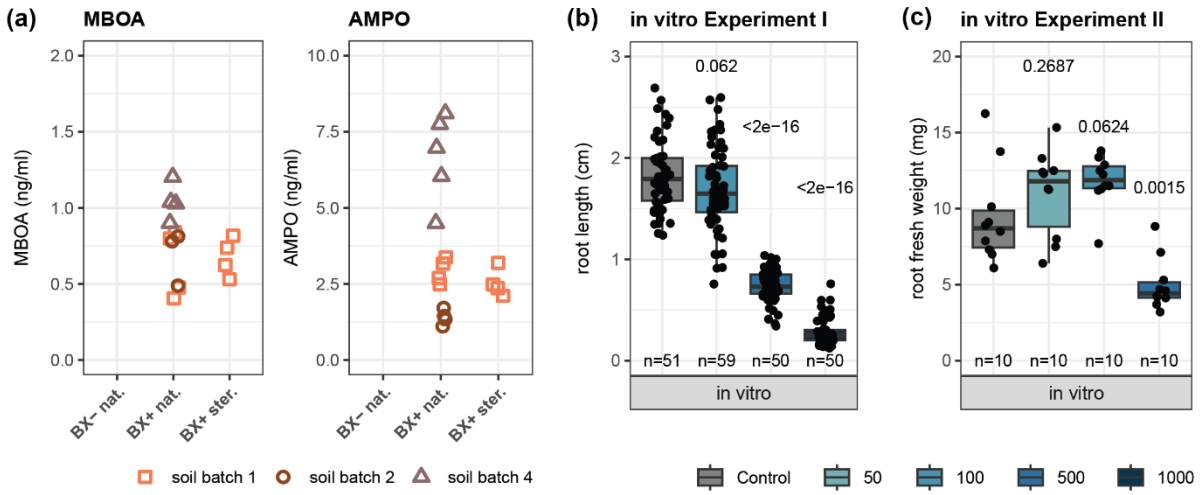

Figure S2 Benzoxazinoid concentrations and Arabidopsis root growth on MBOA supplemented agar plates. **(a)** Concentrations of MBOA and AMPO measured in native as well as sterilized BX-conditioned soils. BX concentrations had been measured in native (nat.) BX_{plus} and BX_{minus} soils for soil batches 1, 2 and 4, and in sterilized (ster.) BX_{plus} soil for soil batch 1; n = 4 for each treatment and soil batch. Samples that were below the detection limit for the given compound are not shown. **(b)** Root length of Arabidopsis germinated and grown for ten days on ½ MS agar plates supplemented with DMSO (Control) or DMSO and increasing amounts of MBOA. **(c)** Root fresh weight of Arabidopsis grown for 21 days in total. Plants were pre-germinated for eight days on ½ MS agar with sucrose, and then grown for an additional 13 days on ½ MS agar plates supplemented with DMSO (Control) or DMSO and increasing amounts of MBOA. For the root fresh weight data, one data point represents the total root fresh weight from five plants grown on one plate. The values shown in the legend represent MBOA concentrations given in µM. The P values on top of each boxplot in (b) and (c) represent the t-test comparison between the Control and the respective MBOA concentration.

15

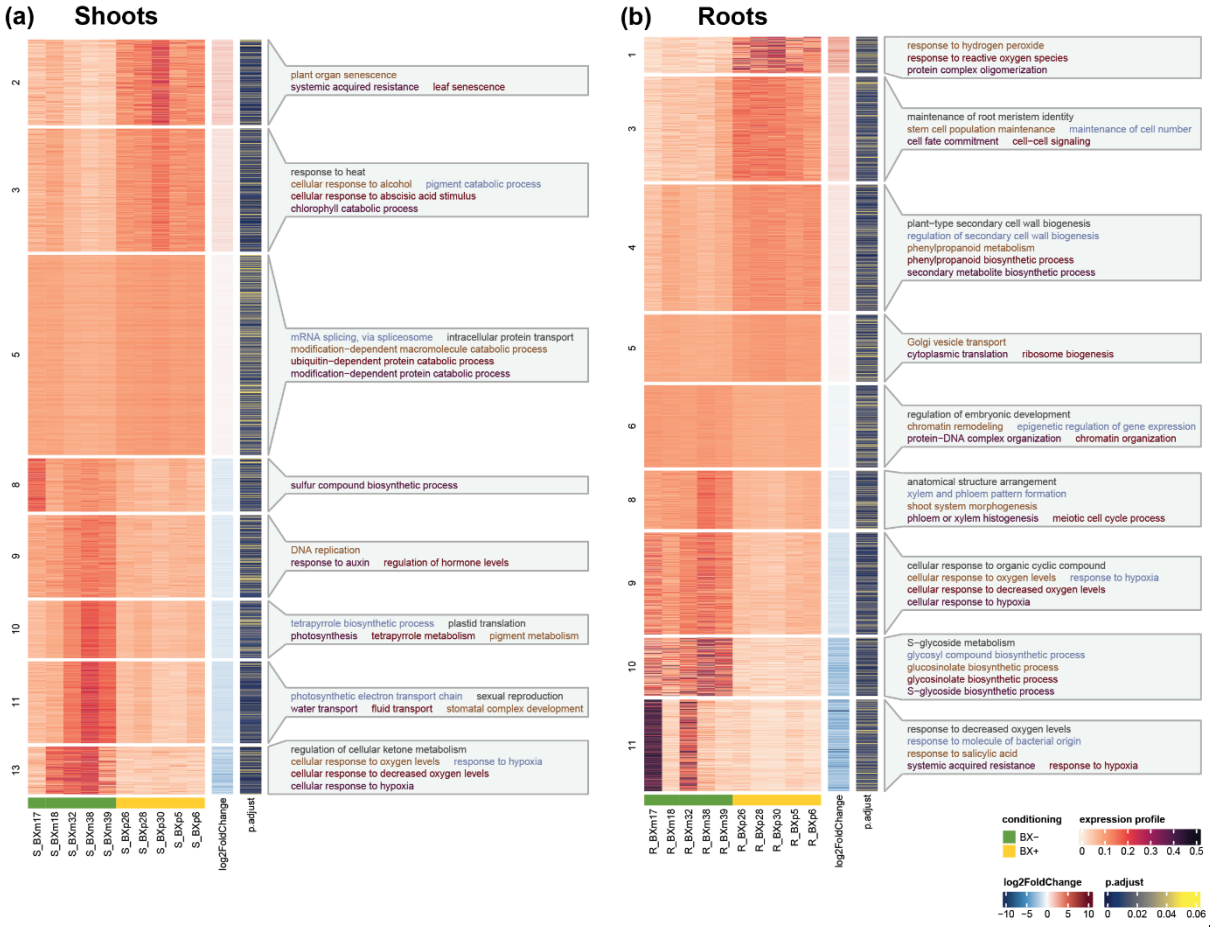

Figure S3 Co-expression analysis of Arabidopsis roots and shoots. Heatmaps of co-expressed gene clusters in (**a**) roots and (**b**) shoots, as identified with coseq. Colors in heatmap correspond to expression profiles i.e., the proportion of normalized counts per gene. Adjacent color bars show the log2FoldChange in expression, as well as the corresponding ajusted P values as inferred with DESeq2. Cluster labels show the top five enriched GO terms (biological processes, P adjusted < 0.01) in the corresponding clusters. The different GO term text colors are for better readability only. Full tables of all enriched GO terms in each cluster in roots and shoots are provided **Tables S7** and **S8**.

16

Supplementary Tables

Table S1 Set up of the different conditioning experiments.

One ‘soil batch’ denotes one independent conditioning experiment, where we used parts of the collected soils indicated in the ‘soil collection’ column, and grew wild-type B73 and *bx1*(B73) maize plants for twelve weeks to condition the soil. Soils were collected from two adjacent Agroscope research fields in Changins, Nyon, Switzerland (46°24'00.0"N 6°14'22.8"E), and the ‘soil collection’ column denotes when the soil was collected and from which field (parcel). For the fertilization, the pots received the specified amount of the respective nutrient solution once per week, starting with a low iron solution for the first four weeks and increasing to a high iron solution for most of the soil batches. rel. hum. = relative humidity, int. = intensity

soil batch	soil collection	pots	growth environment	fertilization	growth conditions
soil batch 1	May 2019 (parcel 29)	2 L (round)	walk-in chamber[1]	4 w. low iron[3], 8 w. high iron[4]	16 h day at 26°C, 8 h night at 23°C, 50% rel. hum., ~550 µmol m^{-2} s^{-1} light int.
soil batch 2	May 2019 (parcel 29)	2 L (round)	walk-in chamber[1]	4 w. low iron, 8 w. high iron	16 h day at 26°C, 8 h night at 23°C, 50% rel. hum., ~550 µmol m^{-2} s^{-1} light int.
soil batch 3	Sept. 2022 (parcel 29/30)	3 L (round)	greenhouse	4 w. low iron, 8 w. high iron	16 h day at min. 23°C, 8 h night at min. 19°C, 300 - 500 µmol m^{-2} s^{-1} light int.
soil batch 4	Sept. 2022 (parcel 29/30)	3 L (round)	Phytotron[2]	12 w. low iron	14 h day at 22°C, 10 h night at 18°C, 60% rel. hum., ~550 µmol m^{-2} s^{-1} light int.
soil batch 5	Aug. 2020 (parcel 30/31)	3 L (round)	greenhouse	4 w. low iron, 8 w. high iron	16 h day at min. 23°C, 8 h night at min. 19°C, 300 - 500 µmol m^{-2} s^{-1} light int.

[1] Kaelte 3000 AG, Landquart, Switzerland
[2] Phytotron Facility, University of Basel, Switzerland
[3] 100 mL of 0.2% Plantaaktiv Typ K (Hauert HBG Duenger AG, Grossaffoltern, Switzerland) and 0.0001% Sequestrene Rapid (Maag, Westland Schweiz GmbH, Dielsdorf, Switzerland)
[4] 200 mL of 0.2% Plantaaktiv Typ K, 0.02% Sequestrene Rapid

Table S2 Set up of the different Arabidopsis experiments.

For each experiment, the soil batch, pot size and growth length are indicated. For details on the soil batch, see Table S1. As measurements, we quantified shoot growth at the end of the experiment, and for certain experiments we additionally recorded the root biomass, collected roots for a microbiota analysis, collected root and shoot material for a transcriptome analysis, or infected the leaves with the fungus *Botrytis cinerea*.

Experiment	Soil batch	Pots	Growth (weeks)	Measurements
Exp. I	soil batch 1	5.5x5 cm (round)	7	Shoot growth
Exp. II	soil batch 1	8x8x8.5 cm (square)	7	Shoot growth
Exp. III	soil batch 1	8x8x8.5 cm (square)	6	Shoot growth, Root microbiota
Exp. IV	soil batch 2	8x8x8.5 cm (square)	6.5	Shoot growth
Exp. V	soil batch 2	6x6x6.5 cm (square)	8	Shoot growth
Exp. V.II	soil batch 2	6x6x6.5 cm (square)	7	Shoot growth, Transcriptome
Exp. VI	Soil batch 3	6x6x6.5 cm (square)	7	Shoot growth, Root biomass
Exp. VII	Soil batch 4	6x6x6.5 cm (square)	7	Shoot growth, Root biomass
Exp. VIII	Soil batch 3	6x6x6.5 cm (square)	6	Shoot growth, *Botrytis* infection
Exp. IX	Soil batch 5	8x8x8.5 cm (square)	5	Shoot growth, *Botrytis* infection
Exp. X	Soil batch 4	8x8x8.5 cm (square)	6	Shoot growth, *Botrytis* infection

Table S3 List of differently abundant bacterial ASVs in soil.

Relative abundance and taxonomic information of differently abundant bacterial ASVs (bASVs) from BX_{plus} and BX_{minus} soil. Due to spatial restrictions, kingdom, phylum and class information are not shown. The mean relative abundances of each bASV in native BX_{plus} and BX_{minus} soil are indicated, ordered by decreasing abundance in the BX_{plus} condition. bASVs with higher abundance in native BX_{plus} soil are shown in bold.

ASV	order	family	genus	abund. BX+	abund. BX–
bASV143	C0119	unassigned	unassigned	0.69%	0.24%
bASV136	Betaproteobacteriales	SC-I-84	unassigned	0.59%	0.35%
bASV105	Sphingomonadales	Sphingomonadaceae	Sphingomonas	0.47%	0.24%
bASV319	Sphingomonadales	Sphingomonadaceae	Sphingomonas	030 %	0.18%
bASV231	Sphingomonadales	Sphingomonadaceae	Sphingomonas	0.27%	0.14%
bASV343	Acidobacteriales	unassigned	unassigned	0.26%	0.14%
bASV199	Sphingomonadales	Sphingomonadaceae	Sphingomonas	0.23%	0.10%
bASV405	Sphingomonadales	Sphingomonadaceae	Sphingomonas	0.23%	0.09%
bASV561	Acidobacteriales	Acidobacteriaceae_(Subgroup_1)	Occallatibacter	0.14%	0.07%
bASV492	Sphingomonadales	Sphingomonadaceae	Sphingomonas	0.13%	0.03%
bASV1079	Xanthomonadales	Rhodanobacteraceae	unassigned	0.09%	0.01%
bASV504	Desulfuromonadales	Desulfuromonadaceae	Desulfuromonas	0.07%	0.21%
bASV1675	Gemmatimonadales	Gemmatimonadaceae	unassigned	0.06%	0.01%
bASV1830	Sphingomonadales	Sphingomonadaceae	Altererythrobacter	0.05%	0%
bASV821	Betaproteobacteriales	Rhodocyclaceae	Dechloromonas	0.04%	0.14%
bASV457	Gaiellales	unassigned	unassigned	0.04%	0.10%
bASV2572	Solibacterales	Solibacteraceae _(Subgroup_3)	Candidatus_ Solibacter	0.03%	0%
bASV1594	Sphingobacteriales	env.OPS_17	unassigned	0.03%	0%
bASV894	Betaproteobacteriales	Rhodocyclaceae	Ferribacterium	0.02%	0.13%
bASV3104	Solibacterales	Solibacteraceae_(Subgroup_3)	Bryobacter	0.02%	0%
bASV1032	Myxococcales	Nannocystaceae	Nannocystis	0%	0.03%
bASV1914	Betaproteobacteriales	Rhodocyclaceae	Candidatus_ Accumulibacter	0%	0.05%
bASV710	Gaiellales	unassigned	unassigned	0%	0.09%
bASV1356	Betaproteobacteriales	Rhodocyclaceae	Azovibrio	0%	0.08%
bASV1762	Desulfuromonadales	Geobacteraceae	Geobacter	0%	0.05%
bASV1781	Gammaproteobacteria_ Incertae_Sedis	Unknown_Family	Acidibacter	0%	0.05%
bASV1821	Gaiellales	unassigned	unassigned	0%	0.04%
bASV3182	Chitinophagales	Saprospiraceae	unassigned	0%	0.02%

Table S4 List of differently abundant bacterial ASVs on roots of Arabidopsis.

Relative abundance and taxonomic information of differently abundant bacterial ASVs (bASVs) of Arabidopsis root communities from native BX_{plus} and BX_{minus} soil. Due to spatial restrictions, kingdom, phylum and class information are not shown. The mean relative abundances of each bASV on roots grown in native BX_{plus} and BX_{minus} soil are indicated, ordered by decreasing abundance in the BX_{plus} condition. bASVs with higher abundance on roots from native BX_{plus} soil are shown in bold.

ASV	order	family	genus	abund. BX+	abund. BX–
bASV39	Betaproteobacteriales	Burkholderiaceae	Massilia	2.08%	0.59%
bASV44	Betaproteobacteriales	Burkholderiaceae	Rubrivivax	0.63%	1.30%
bASV511	Sphingobacteriales	env.OPS_17	unassigned	0.20%	0.02%
bASV453	Solirubrobacterales	67-14	unassigned	0.11%	0.01%
bASV698	Myxococcales	Sandaracinaceae	unassigned	0.02%	0.10%
bASV138	Cellvibrionales	Cellvibrionaceae	Cellvibrio	0.01%	0.28%
bASV117	Betaproteobacteriales	Burkholderiaceae	Massilia	0.01%	0.78%
bASV830	Betaproteobacteriales	Burkholderiaceae	unassigned	0%	0.09%
bASV1246	Myxococcales	Sandaracinaceae	Sandaracinus	0%	0.06%
bASV164	Betaproteobacteriales	Burkholderiaceae	Massilia	0%	0.59%
bASV791	Spirochaetales	Spirochaetaceae	Spirochaeta_2	0%	0.10%
bASV1445	Xanthomonadales	Rhodanobacteraceae	unassigned	0%	0.05%

The **Supplementary Tables S5 to S8** are in a common excel file with the following work sheets:

Table S5 Shoot transcriptome

List of significantly differentially expressed genes ($P_{adj} < 0.05$, , log2FoldChange ±>1) in shoots as inferred with DESeq2. The work sheet lists the Gene-ID, its base mean of expression, the log2 fold change and its standard error, the DESeq statistic, its P value and adjusted P value.

Table S6 Root transcriptome

List of significantly differentially expressed genes ($P_{adj} < 0.05$, log2FoldChange ±>1) in roots as inferred with DESeq2. The work sheet lists the Gene-ID, its base mean of expression, the log2 fold change and its standard error, the DESeq statistic, its P value and adjusted P value.

Table S7 Shoot co-expression analysis

The table lists for shoots for each cluster of co-expressed genes the enriched GO terms with their ID, the description (biological processes), its gene ratio, the background gene ratio, its P value, adjusted P value and Q value together with the IDs of the identified genes and their count per cluster.

Table S8 Root co-expression analysis

The table lists for roots for each cluster of co-expressed genes the enriched GO terms with their ID, the description (biological processes), its gene ratio, the background gene ratio, its P value, adjusted P value and Q value together with the IDs of the identified genes and their count per cluster.

Table S9 List of genes mentioned in the text for RNASeq results

List of exemplary genes differentially regulated in shoots and roots of Arabidopsis grown on BX_{plus} compared to BX_{minus} soil. Genes are sorted by tissue (shoots, roots) and by regulation (upregulated in tissue grown on BX_{plus} soil, downregulated in tissue grown on BX_{plus} soil). For each gene, the cluster affiliation as well as the log2 fold change (Log2FC) of the gene expression and the adjusted P value for the differential expression on BX_{plus} versus BX_{minus} are indicated.

Genes in shoots, upregulated (BX_{plus} > BX_{minus})

Gene name	Locus	cluster	Log2FC	adjusted P value
NFYA5	AT1G54160	cluster 3	1.27	< 0.0001
AKS1	AT1G51140	cluster 3	1.02	< 0.0001
PR5	AT1G75040	cluster 2	1.28	0.03
PR2	AT3G57260	cluster 2	1.75	0.002

Genes in shoots, downregulated (BX_{plus} < BX_{minus})

Gene name	Locus	cluster	Log2FC	adjusted P value
LHCB6	AT1G15820	cluster10	-1.25	0.003
RBCS1A	AT1G67090	cluster10	-1.3	0.006
CHLI2	AT5G45930	cluster10	-1.04	0.003
TN8	AT1G72910	cluster 13	-1.83	0.0008
TN9	AT1G72920	cluster 13	-2.60	< 0.0001
TAA1	AT1G70560	cluster 9	-1.02	< 0.0001
LAX3	AT1G77690	cluster 9	-1.06	0.002

Genes in roots, upregulated (BX_{plus} > BX_{minus})

Gene name	Locus	cluster	Log2FC	adjusted P value
MYB66/WER	AT5G14750	cluster 3	1.24	0.02
MYB23	AT5G40330	cluster 3	1.47	0.002
PRR1	AT1G32100	cluster 4	1.26	< 0.0001
MYB43	AT5G16600	cluster 4	1.10	0.0001
SWEET4	AT3G28007	cluster 1	3.22	0.004
SWEET12	AT5G23660	cluster 1	2.73	0.0003

Genes in roots, downregulated (BX_{plus} < BX_{minus})

Gene name	Locus	cluster	Log2FC	adjusted P value
MKK7	AT1G18350	cluster 11	-4.72	0.02
WRKY40	AT1G80840	cluster 11	-2.68	0.02
CRK9	AT4G23170	cluster 11	-3.75	0.005
TN7	AT1G72900	cluster 11	-2.74	0.001
TN8	AT1G72910	cluster 11	-4.31	< 0.0001
FMO GS-OX1	AT1G65860	cluster 10	-1.71	0.03
IMD1	AT5G14200	cluster 10	-2.00	0.01

Supplementary Datasets

Dataset S1 Microbiota analysis

The Dataset S1 presents the R markdown output of the microbiota analysis. The raw sequencing data is available from ENA, the input data, R code and R markdown output are available from GitHub under https://github.com/PMI-Basel/Stengele_et_al_At_BX-feedbacks.

Dataset S2 Transcriptome analysis

The Dataset S2 presents the R markdown output of the transcriptome analysis. The raw sequencing data is available from ENA, input data, R code and R markdown output are available from GitHub under https://github.com/PMI-Basel/Stengele_et_al_At_BX-feedbacks.